Published in "Organometallics 30(22): 6119–6132, 2011"
which should be cited to refer to this work.

Modulating the Steric, Electronic, and Catalytic Properties of Cp* Ruthenium Half-Sandwich Complexes with β-Diketiminato Ligands

Andrew D. Phillips,[†,‡] Katrin Thommes,[†] Rosario Scopelliti,[†] Claudio Gandolfi,[§] Martin Albrecht,[‡,§] Kay Severin,[†] Dominique F. Schreiber,[‡] and Paul J. Dyson*[,†]

[†]Institut des Sciences et Ingénierie Chimiques, Ecole Polytechnique Fédérale de Lausanne (EPFL), CH-1015 Lausanne, Switzerland
[‡]School of Chemistry and Chemical Biology, University College Dublin, Belfield, Dublin 4, Ireland
[§]Department of Chemistry, University of Fribourg, Chemin du Musée 9, CH-1700 Fribourg, Switzerland

ABSTRACT: Five different types of β-diketiminate ligands, bearing electron-donating to strongly electron-withdrawing substituents, were synthesized and used in the synthesis of Cp* ruthenium complexes (Cp* = η^5-C_5Me_5). One series consists of complexes with a covalent Ru^{III}−Cl bond, and the other series features a reduced Ru^{II} center, where the chloride is abstracted by treatment of the corresponding Ru^{III} compounds with Zn or Mg. All compounds were characterized by single-crystal X-ray diffraction, UV−visible spectroscopy, and cyclic voltammetry. In the case of Ru^{II} complexes, solution NMR techniques provided key information regarding the electronic and structural differences induced by the different β-diketiminate ligands employed. Capitalizing on the facile reduction−oxidation cycle of the Cp* ruthenium β-diketiminato complexes, catalytic atom transfer radical addition (ATRA) and cyclization (ATRC) reactions were performed on relevant substrates. The turnover rates are strongly dependent on the type of β-diketiminate used, where ligands with electron-withdrawing substituents, i.e., trifluoromethyl groups, provided complexes that efficiently catalyze the addition of CCl_4 or toluenesulfonyl chloride to styrene. In contrast, complexes with electron-donating substituents on the β-diketiminate promoted efficient ATR cyclization of *N*-allyl-*N*-phenyltrichloroacetamide and 2,2,2-trichloroethyl ether. Thus, the overall product conversion and yield are dependent on matching the ligand substitution pattern of the catalyst to the type of substrate.

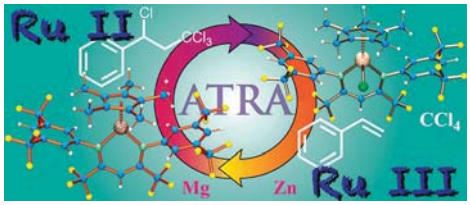

INTRODUCTION

Organoruthenium complexes promote a range of catalytic reactions such as olefin metathesis,[1] C−H activation,[2] hydrogenation,[3] and oxidation.[4] A key advantage of using Ru over other metals is the strong preference for coordinating and activating olefinic bonds,[1b] which in turn reduces or eliminates the requirement for functional group protection. Although complexes containing phosphine or carbene ligands currently dominate the organoruthenium field, the past decade has witnessed a renewed interest in complexes bearing strongly donating nitrogen chelates.[5] A well-known example is the Noyori transfer hydrogenation catalyst, featuring the tosylethylenediamine ligand.[6] This expanding field now includes organometallic species featuring anionic N,N′-chelates, where a number of complexes with the amidinate ligand have been reported[7] (Figure 1a). The five-membered β-diketiminates (Figure 1b) have also received considerable attention[8] and continue to be successfully employed in stabilizing low-coordinate and highly reactive main-group[9] and transition-metal[10] complexes. In particular, this class of ligand exerts considerable steric effects originating from the functional groups on the N-flanking positions, normally aryl substituents. Thus, the β-diketiminate ligand encloses and partially encapsulates the central metal, preventing dimerization or oligomerization. In β-diketiminato complexes featuring a higher metal coordination number,

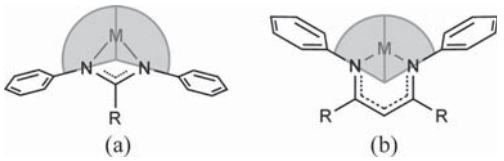

Figure 1. Amidinates (a) and β-diketiminates (b) as anionic N,N′-chelate ligands. The gray regions indicate the bite angle of the corresponding ligand.

significant interligand repulsion is often observed. In contrast, only minor steric interactions are encountered in species bearing an amidinate ligand, where the N-flanking substituents are folded away from the metal.

The chemistry of first-row transition metal based β-diketiminate compounds is quite advanced, with numerous known examples, while comparatively, the variety of complexes associated with the second- and third-row d-block metals is far less explored. Nevertheless, β-diketiminato complexes of Zr,[11] Nb,[12] Mo,[13] Ag/Au,[14] Pd/Pt,[15,16] and Rh/Ir[17,18] have recently emerged. Concurrently a large expansion in the number of catalytic applications employing β-diketiminate transition-metal complexes is in progress. In particular, the fields of polymerization,[19]

Scheme 1. Bifunctional Metal–Ligand Reactions of the η^6-Arene β-Diketiminato Ruthenium Complex 1 with Acetylene, Ethylene, Styrene, and Dihydrogen, Forming Species Featuring a Chelating β-Diimine Ligand

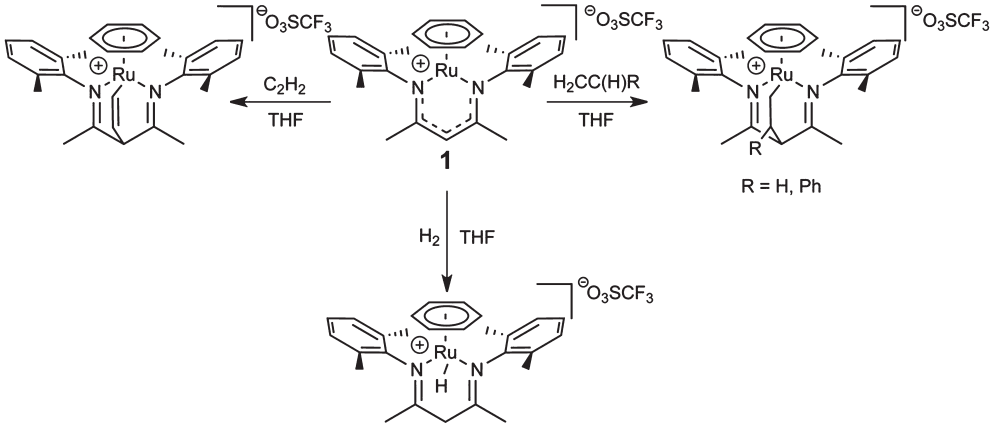

oxidation,[20] olefin metathesis,[13] hydrogenation,[17a,21] and hydroamination[22] have witnessed significant developments. Recently we described the synthesis and characterization of the first β-diketiminato ruthenium complexes supported by neutral η^6-arene ligands.[23] The coordinatively unsaturated complex **1** (Scheme 1) was found to display an unusual metal–ligand bifunctional character, as evidenced in reactions with alkenes and alkynes, which undergo reversible metal–ligand cycloadditions. Furthermore, a rare example of heterolytic cleavage of dihydrogen involving the nucleophilic β-carbon center of the β-diketiminate was observed, resulting in an efficient catalyst for the hydrogenation of highly substituted olefins, including 1-methylcyclohexene and 4-isopropenyl-1-methylcyclohexene.

Herein, we expand the chemistry of organoruthenium compounds bearing a β-diketiminate ligand, by describing a new series of [Cp*Ru^{III}(β-diketiminato)Cl] and [Cp*Ru^{II}(β-diketiminato)] complexes. A detailed analysis of the steric and electronic effects imparted by differently substituted β-diketiminates and the influence of this ligand class on the catalytic activity of the Ru^{III} complexes in atom transfer radical addition (ATRA) and cyclization (ATRC) reactions is also described.

RESULTS AND DISCUSSION

Synthesis and Reactivity of Complexes 7–17. The protonated β-diketiminates used in this study are known compounds and were prepared via reported literature methods.[24] In order to facilitate metal binding, deprotonation of the ligand to the corresponding conjugate lithium salts **2–6** was accomplished using *n*-BuLi in *n*-pentane (see Scheme 2).[25]

Scheme 2. Synthetic Routes Used To Prepare the β-Diketiminate Ligands with Electron-Donating (2, 3) or Electron-Withdrawing Groups (4–6) and the Corresponding Lithium Salts

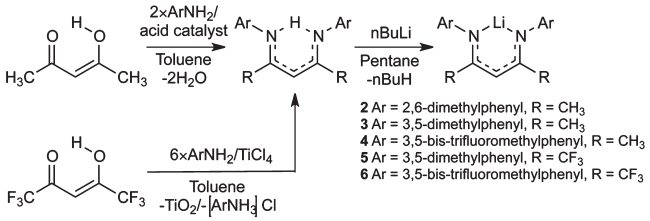

Subsequently, the series of β-diketiminato ruthenium(III) complexes **7–11** were prepared using an established methodology previously employed in the synthesis of **1**.[23] A CH_2Cl_2 solution of the corresponding β-diketiminato lithium complex (**2–6**) was added slowly to a solution of the dimer [Cp*Ru^{III}Cl$_2$]$_2$ in CH_2Cl_2 (Scheme 3). During some reactions the formation of a byproduct was observed, which was particularly dominant in the case of **11** (Scheme 4). The identity of this species **12**, was confirmed by single-crystal X-ray diffraction analysis, which showed a metal-coordinated neutral 1,2,3,4-tetramethylfulvene ligand, containing one exocyclic and two internal C=C bonds.[26]

The byproducts of type **12** formed in the synthesis of **7–11** were removed by washing with pentane, and residual [Cp*Ru^{III}Cl$_2$]$_2$ was removed with diethyl ether. To increase the yield of **11**, an alternative method was employed. Recently, the synthesis of the dimeric silver acetonitrile complex **18** (Scheme 5), featuring the fluorinated β-diketiminate **6**, was reported.[14a] Species **18** bearing the β-diketiminate **6** proved to be a highly valuable and versatile ligand-transfer reagent. Reaction of **18** with [Cp*Ru^{III}Cl$_2$]$_2$ afforded **11** in 87% yield (Scheme 5) without the formation of **12**. Alternatively, transmetalation of the fluorinated β-diketiminato thallium complex **19** with the [Cp*Ru^{III}Cl$_2$]$_2$ dimer also provided **11** in high yield (Scheme 5). This approach has been previously used to prepare Ni and Mo β-diketiminato complexes.[13,27] The procedure for preparing the thallium precursor is based on that reported by Grubbs et al.[28] and others.[29] Complex **19** was first prepared and isolated from the reaction between TlOEt and **6** and subsequently reacted with [Cp*Ru^{III}Cl$_2$]$_2$ in CH_2Cl_2 to afford **11** (Scheme 5) without any evidence for the formation of **12**.

In the solid state, all of the Ru^{III} complexes are stable toward O_2, but when they are dissolved in nondegassed solvents, the complexes decompose within hours, except for **10** and **11**, which are stable for several months even in solution.

Complexes **7–11** are readily transformed into the corresponding Ru^{II} species **13–17** in high yield by reduction with zinc or magnesium in dry and degassed THF (Scheme 3). Extraction with *n*-pentane and filtration through Celite provided the Ru^{II} compounds in pure form, as determined by ^{1}H and ^{13}C NMR spectroscopy. An alternative method for the synthesis of a [Cp*Ru^{II}(β-diketiminato)] complex was reported by Russell et al.[30] and involves the direct reaction of [Cp*Ru^{III}Cl$_2$]$_2$ with the protonated phenyl-substituted β-diketiminate in the presence of excess K_2CO_3. The reaction

Scheme 3. Synthesis of the Ru^{III} Complexes 7−11 and the Ru^{II} Complexes 13−17

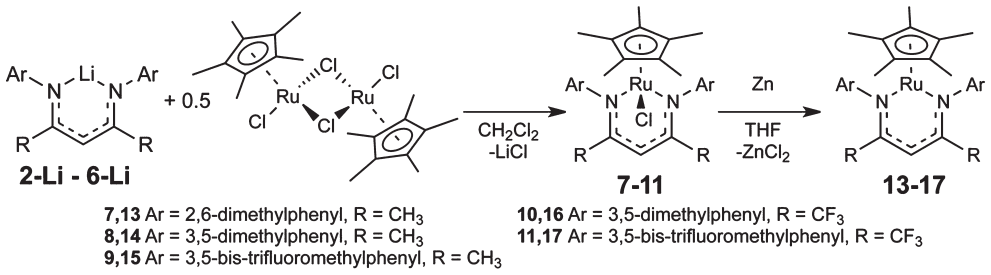

Scheme 4. Synthesis of the Ru^{III} Complex 11 and the Corresponding Byproduct 12

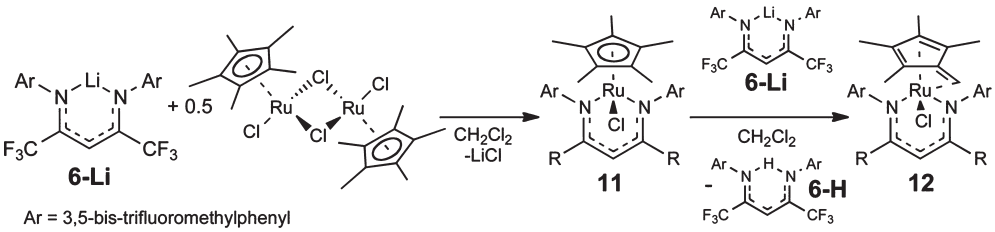

Scheme 5. Alternative Routes to the Synthesis of Complex 11

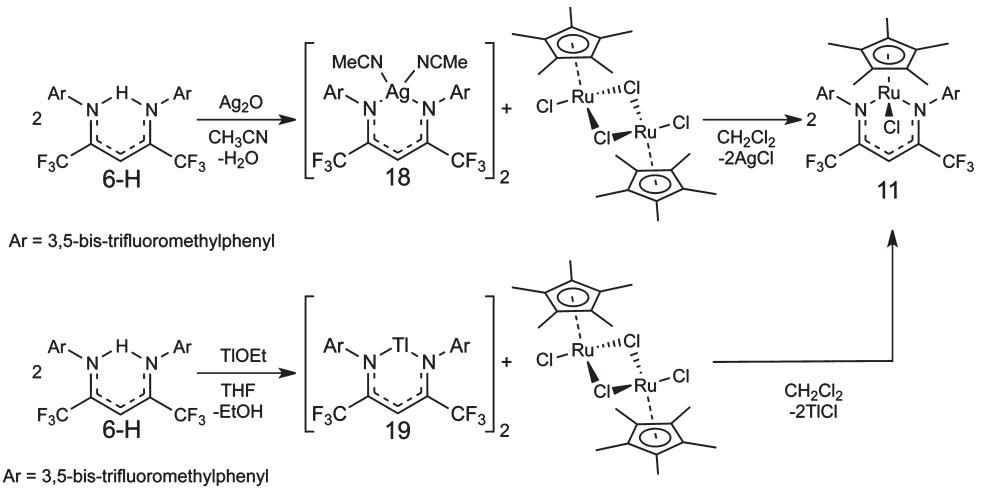

presumably proceeds with the in situ formation of $[Cp^*Ru^{II}(\mu_2\text{-}OCH_3)]_2$, a valuable precursor to a diverse range of complexes bearing the Cp^*Ru^{II} fragment. The synthesis is completed by nucleophilic addition of the phenyl-substituted β-diketiminate and loss of methanol.[31]

Upon exposure to chlorinated solvents such as CH_2Cl_2, $CHCl_3$, and CCl_4, complexes **13**−**17** rapidly convert to the original Ru^{III} species **7**−**11**, as determined by ESI-MS and UV−visible experiments. Similar behavior has been observed for other Ru^{II} complexes, including Cp^*Ru^{II} amidinate complexes [32] and the family of Cp^*Ru^{II} acetylacetone compounds.[31] All five β-diketiminato Ru^{II} complexes reported here are stable in wet degassed hydrocarbon solvents: i.e., THF, Et_2O, and pentane. However, all Ru^{II} species react spontaneously with dioxygen, both in the solid state and in nondegassed solutions, which prevented accurate elemental analyses of the complexes.

Spectroscopic Characterization of Complexes 7−11 and 13−17. A comparison of the ^1H and ^{13}C NMR spectra of **13**−**17** reveals that the electronic effects exerted by the different β-diketiminato ligands are readily distinguished, with the compounds featuring electron-deficient ligands, i.e., **16** and **17**, exhibiting increased shielding of the ring carbon atoms. For all Ru^{II} complexes a single resonance for the methyl substituents associated with the η^5-C_5Me_5 ligand is observed, indicating that in solution unhindered rotation occurs. The combined effects for the induced structural distortions in the η^5-C_5Me_5 ligand and electronic influences imparted by the Ru-β-diketiminate fragment are difficult to quantify separately. Complex **17** has the greatest number of CF_3 substituents on the β-diketiminato ligand, which corresponds to the highest shielded $\delta(^1H)$ value of the Cp* methyl groups (Table 1). Conversely, **14** has the sterically least hindered β-diketiminate, with 3,5-bis-methylphenyl flanking aryls, and has the least shielded $\delta(^1H)$ values for CH_3 groups associated with the Cp* ring, indicating a decrease in electron density for this ligand in **14** compared to that in **17**. For species **16** and **17** with CF_3 substituents in the α-positions, a large increase for the $\delta(^1H)$ values of the β-CH position is observed, which correlates with greater π-electron delocalization within the core atoms of the β-diketiminate ligand. Since the extended π-type molecular orbitals are orthogonal to the plane of the ligand, contraction of the σ-bonding ligand framework, originating from electron-withdrawing

Table 1. Selected ^{1}H and ^{13}C NMR Data for the Ru^{II} Complexes 13−17[a]

	Ar	R	$\delta(^{1}H)$ β-CH	$\delta(^{13}C)$ β-CH	$\delta(^{13}C)$ α-C	$\delta(^{1}H)$ $(C_5(CH_3)_5)$	$\delta(^{13}C)$ $(C_5(CH_3)_5)$	$\delta(^{13}C)$ $(C_5(CH_3)_5)$
13	2,6-$(CH_3)_2C_6H_3$	CH_3	5.455	98.86	157.52	0.938	9.98	77.16
14	3,5-$(CH_3)_2C_6H_3$	CH_3	5.553	98.13	157.36	1.243	10.03	77.74
15	3,5-$(CF_3)_2C_6H_3$	CH_3	5.294	99.28	157.97	0.864	9.67	78.15
16	3,5-$(CH_3)_2C_6H_3$	CF_3	7.080	90.24	145.78	0.973	9.25	83.42
17	3,5-$(CF_3)_2C_6H_3$	CF_3	6.714	91.33	146.27	0.476	8.81	84.39

[a]Compounds were dissolved in C_6D_6 and spectra recorded at 25 °C.

inductive effects, results in an increased π-orbital overlap. Similarly, CF_3-substituted aryls have been used to decrease the atomic orbital size of heavy main-group elements, resulting in strengthened P═N and As═N π-bonds.[33]

A direct electronic comparison of the Ru^{III} and Ru^{II} complexes is possible using UV−visible spectroscopy. Spectra of the blue and green Ru^{III} complexes were measured in CH_2Cl_2, while *n*-pentane was used for the more reactive magenta and red Ru^{II} species. In both the Ru^{III} series **7**−**11** (Table 2) and Ru^{II} series **13**−**17** (Table 3), depending on the

Table 2. UV−Visible Absorptions for the Ru^{III} Complexes 7−11[a]

complex	λ_{max}(A) (nm)	$10^3\varepsilon$ (M^{-1} cm^{-1})	λ_{max}(B) (nm)	$10^3\varepsilon$ (M^{-1} cm^{-1})	λ_{max}(C) (nm)	$10^3\varepsilon$ (M^{-1} cm^{-1})
7	646	4.4			318	20.3
8	637	5.5			318	27.6
9	636	5.1			322	28.5
10	606	4.0	410	8.2	349	26.8
11	586	3.5	420	9.6	345	24.7

[a]Spectra were recorded at 25 °C in CH_2Cl_2.

Table 3. UV−Visible Absorptions for the Ru^{II} Complexes 13−17[a]

complex	λ_{max}(A) (nm)	$10^3\varepsilon$ (M^{-1} cm^{-1})	λ_{max}(B) (nm)	$10^3\varepsilon$ (M^{-1} cm^{-1})	λ_{max}(C) (nm)	$10^3\varepsilon$ (M^{-1} cm^{-1})
13	531	1.1			306	40.2
					322	40.1
14	516	1.8			308	50.1
15	517	1.9	387	6.3	314	53.0
16	*b*		447	7.7	317	34.0
17	*b*		448	8.5	318	36.0

[a]Spectra were recorded at 25 °C in *n*-pentane. [b]The λ_{max}(A) band is broad and is merged at the base with the λ_{max}(B) transition.

substitution pattern of the β-diketiminate ligand, either two or three sets of absorption maxima, λ_{max}(A−C), were observed. Assignment of the absorption bands to electronic transitions is based on previous studies involving ruthenium coordination compounds with unsaturated chelating nitrogen ligands, in particular 1,3-diazabutadienes,[34] and employing high-level time-dependent density functional theory (TD-DFT) calculations using the B3LYP level of theory (a full discussion is given in the Supporting Information). The first set of absorptions, λ_{max}(A) in the Ru^{III} series, corresponds to a mixture of d−d transitions and LMCTs originating from the β-diketiminate ligand to the metal center. In contrast, for the Ru^{II} complexes, these λ_{max}(A) bands are assigned as pure d−d-centered transitions, as indicated by the relatively small molar extinction coefficients in the range of $(1.1-1.9) \times 10^3$ M^{-1} cm^{-1}. For **13** and **14**, the wavelength associated with λ_{max}(A) is longer and corresponds to less energetic d−d transitions. For **16** and **17** with α-CF_3 substituents, the d−d transitions are significantly broadened with no discernible maximum. For the Ru^{III} complexes, a second set of absorptions, labeled λ_{max}(B), was observed when the β-diketiminate has α-CF_3 substituents. This band corresponds to a charge transfer from the Cl ligand to the metal center, termed XMCT, commonly seen in Ru complexes featuring 1,3-diazabutadiene-type ligands.[34a,35] Similarly, TD-DFT calculations predict that this transition occurs at lower wavelength for the Ru^{III}−Cl complexes with α-CH_3 substituents, i.e., **7**−**9**, but are combined with other LMCT bands associated with λ_{max}(C). For the Ru^{II} series, λ_{max}(B) is only observed for complexes featuring CF_3 α-substitution, i.e., **16** and **17**, which according to the models corresponds to a MLCT between the Ru center and the β-diketiminate ligand. The most intense band present in the spectra of all complexes, labeled λ_{max}(C), is associated with LLCTs associated with the π system of the β-diketiminate. However, some high-energy LMCTs are also present and mixed with the LLCTs, especially for Ru^{II} and Ru^{III} complexes featuring α-CH_3 groups on the β-diketiminate ligand. In general, for both series of complexes, λ_{max}(C) undergoes a bathochromic shift corresponding to increasing electron-withdrawing character of the β-diketiminate ligand, where both the Ru^{III} (**11**) and Ru^{II} (**17**) species feature less energetic LMCTs. This is consistent with the TD-DFT calculated models, which suggest that the nature of the LUMO in the electron-donating CH_3 α-substituted β-diketiminate complexes, i.e., **7** and **13**, are largely metal-based, whereas for **11** and **17**, featuring electron-withdrawing CF_3 groups, the LUMO is predominately built on contributions from the π-type orbitals from core atoms of the β-diketiminate ligand.

Solid-State Characterization of Complexes 7−17. Comprehensive structural characterization of all the complexes was accomplished using X-ray diffraction methods. This enables a detailed analysis of the influence imparted by different substitution patterns for the β-diketiminate ligands employed (Figures 2−7 and Tables 4 and 5). The Ru^{III} species with an additional Cl ligand, **7**−**11**, feature a distorted three-legged piano-stool geometry with the flanking aryl groups of the β-diketiminate ligand positioned parallel with the plane of the η^5-C_5Me_5 group. Depending on the type of β-diketiminate ligand used, some notable structural variations are observed, especially for the Ru^{III} complexes. Similarly to the previously reported η^6-C_6H_6 substituted chloro β-diketiminato Ru^{II} complexes,[23c] two distinctive conformations of the coordinated β-diketiminate ligand are apparent (Figure 8). The first type of conformation, associated primarily with **7**, and to a lesser extent **8**, shows the β-diketiminate ligand folded along the N−N′ vector and, albeit less pronounced, orthogonally folded along the Ru−C $_\beta$ vector. The maximum amount of N−N′ folding, as indicated by the Ru−N,N′$_{bisection}$−C $_\beta$ angle, defined

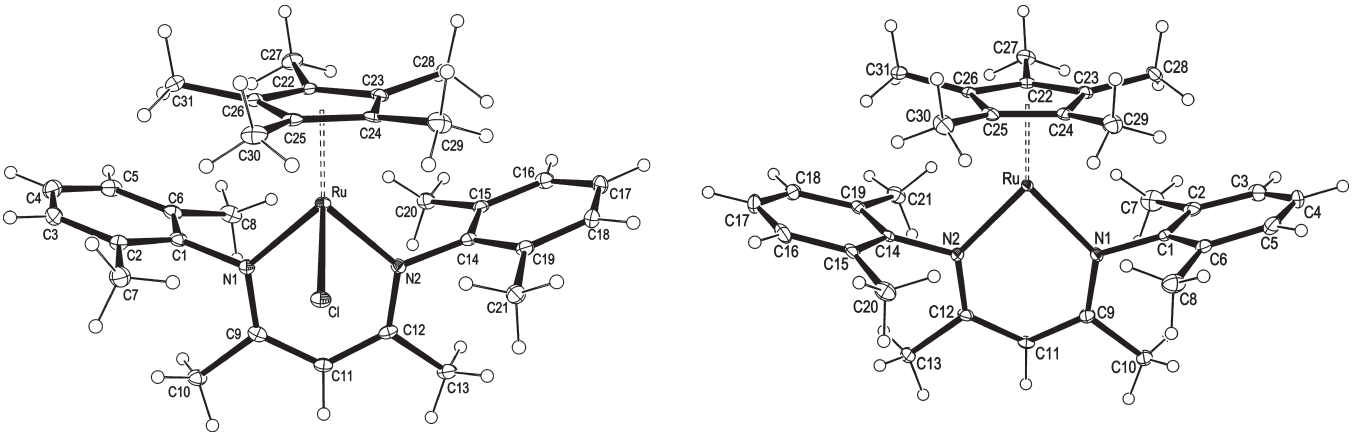

Figure 2. ORTEP diagram of the Ru^{III} complex **7** (left) and the Ru^{II} complex **13** (right) with the 2,6-$(CH_3)_2C_6H_3$-α-CH_3 β-diketiminate, drawn with 30% probability ellipsoids. Disordered sections of the molecule and solvates are omitted for clarity.

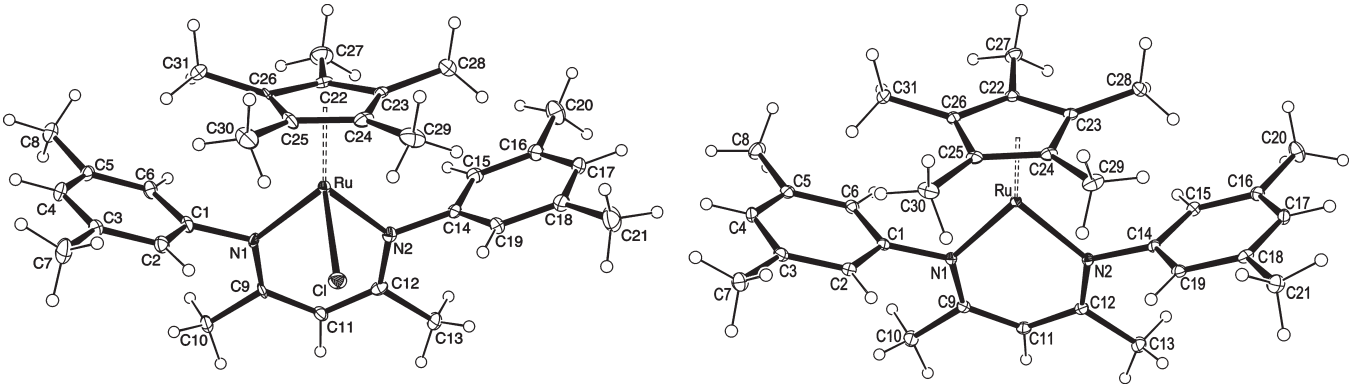

Figure 3. ORTEP diagram of the Ru^{III} complex **8** (left) and the Ru^{II} complex **14** (right) with the 3,5-$(CH_3)_2C_6H_3$-α-CH_3 β-diketiminate, drawn with 30% probability ellipsoids. Disordered sections of the molecule and solvates are omitted for clarity.

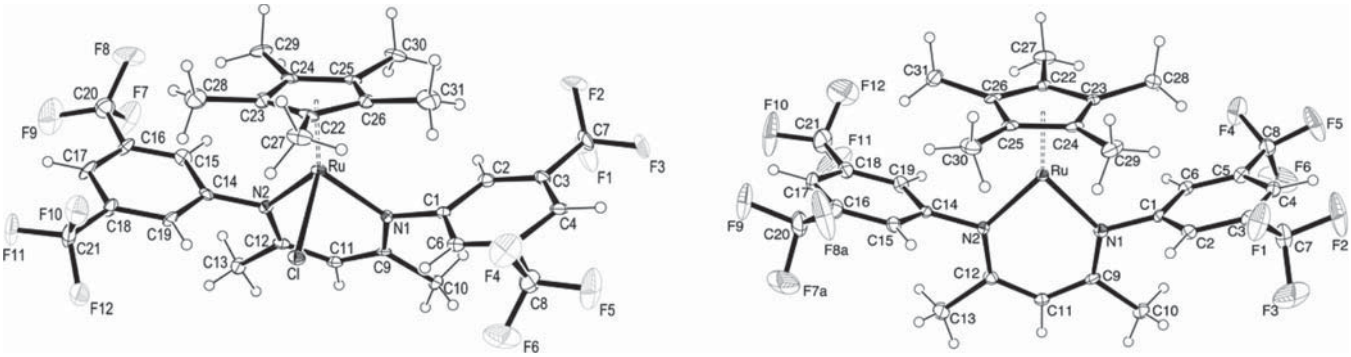

Figure 4. ORTEP diagram of the Ru^{III} complex **9** (left) and the Ru^{II} complex **15** (right) with the 3,5-$(CF_3)_2C_6H_3$-α-CH_3 β-diketiminate, drawn with 30% probability ellipsoids. For **9**, only one of the unique molecules in the unit cell is shown. Disordered sections of the molecule and solvates are omitted for clarity.

by θ in Figure 8, is largest in species **7** due to the steric hindrance originating from *o*-CH_3 groups attached to the flanking aryls. In contrast, complexes bearing CF_3 substituents at the α-position or aryl groups on the β-diketiminato ligand have an essentially planar core framework, as indicated by $\theta >$ 170°. This structural dichotomy between the two types of Ru^{III} complexes defines the extent of π-electron delocalization between the central atoms of the β-diketiminato ligand and the Ru center. For example, in the case of **7**, a more localized allylic π-type interaction is envisaged between the p_π orbitals of the N centers and the Ru d_{xz} orbital. However, for species **9**–**11**, an extended π-delocalized MO involving the metal and the entire β-diketiminato framework, including the C═N and C═C bonds, is apparent. The effect of adding electron-donating or -withdrawing groups to the β-diketiminate ligand is directly manifested in the magnitude of the Ru–Cl bond length (Table 4), with **7** showing the longest distance within the series. As expected, both **10** and **11** with the electron-withdrawing α-positioned CF_3 groups possess the shortest Ru–Cl bonds of the series. Complex **9**, with *m*-CF_3 groups on the aryl

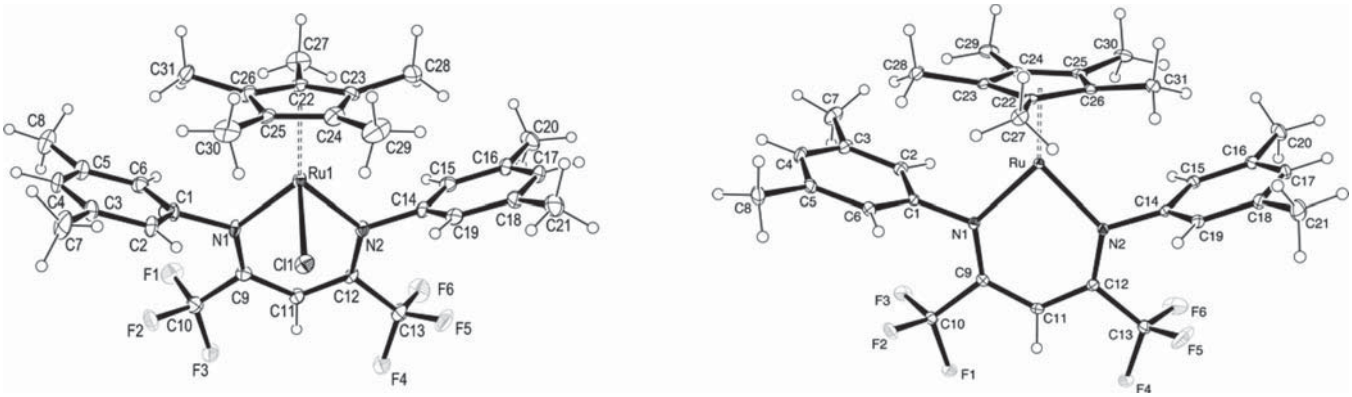

Figure 5. ORTEP diagram of the Ru^{III} complex **10** (left) and the Ru^{II} complex **16** (right) with the 3,5-$(CH_3)_2C_6H_3$-α-CF_3 β-diketiminate, drawn with 30% probability ellipsoids. Disordered sections of the molecule and solvates are omitted for clarity.

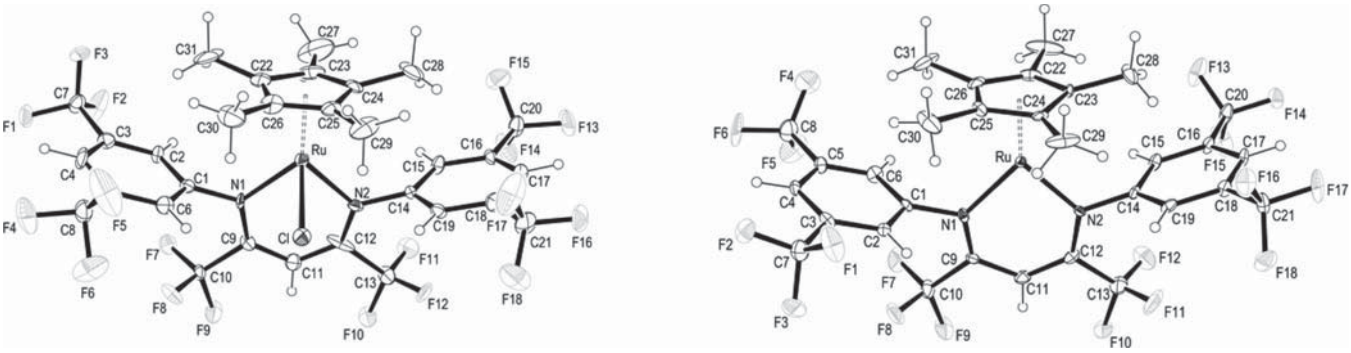

Figure 6. ORTEP diagram of the Ru^{III} complex **11** (left) and the Ru^{II} complex **17** (right) with the 3,5-$(CF_3)_2C_6H_3$-α-CF_3 β-diketiminate, drawn with 30% probability ellipsoids. Disordered sections of the molecule and solvates are omitted for clarity.

substituents, has a slightly longer Ru−Cl bond distance than the species with α-positioned CF_3 groups. Similar trends for Ru−Cl bond lengths are also observed for the $(\eta^6$-$C_6H_6)$RuCl complexes with CF_3-substituted β-diketiminates.[23c]

A number of reports have shown the strong steric influence of the β-diketiminate ligand, and for the complexes described herein, the Ru−Cp*(centroid) distance provides a useful indicator for this steric interaction. Interestingly, species **11** has a Ru−Cp*(centroid) distance equal to that of **7**, whereas the Ru−N distances in **11** are significantly shorter than in **7** (Table 4), which suggests that steric interactions between the Cp* ring and flanking aryl substituents of the β-diketiminate ligand are maximized in this particular species. For those complexes bearing CH_3 α-substituted β-diketiminates, i.e., **7**−**9**, the N−Ru−N bond angles are smaller than those in **10** and **11** with α-CF_3 groups. The internal C_β−C_α bond lengths associated with the β-diketiminate ligand are also significantly decreased in **11** compared to the other compounds in the series.

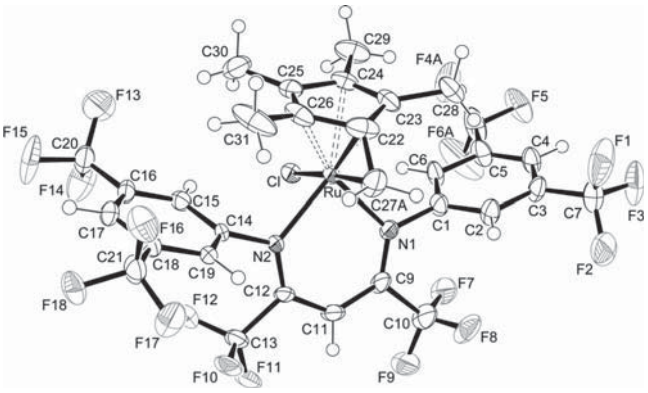

Figure 7. ORTEP diagram of Ru^{II} complex **12** featuring the tetramethyl-substituted fulvene ligand, drawn with 50% probability ellipsoids. Disordered sections of the molecule, including the overlap of complex **11**, are omitted for clarity.

The secondary product **12**, formed during the reaction involving **11** (Scheme 2), was crystallized from *n*-pentane by slow evaporation, and the crystals were found to contain both **11** and **17** in a ratio of 4:6. Consequently, the bond parameters should be treated with caution. However, the structure of **17** (Figure 7) reveals the alternating C═C double and C−C single bonds associated with the fulvene ligand. Characteristically, the exocyclic CH_2 group is bent toward the Ru center, forming a η^2-Ru−C═C π bond as observed in other related organoruthenium systems bearing this ligand type.[26]

The corresponding series of reduced Ru^{II} complexes **13**−**17**, in which the Cl ligand is absent, are characterized by a planar structure with C_{2v} symmetry, when considering only the core framework of the β-diketiminato ligand and chelated metal. This topology is evident from the Ru−N,$N'_{bisection}$−C_β bond angle θ, which for the entire Ru^{II} series is greater than 176°. Moreover, the flanking aryl groups are positioned parallel to the ring plane of the Cp* ligand. Similarly, cationic $(\eta^6$-$C_6H_6)Ru^{II}$ β-diketiminate complexes such as **1** have structurally identical features: i.e., a planar β-diketiminato ligand with an orthogonally aligned η^6-arene group.[23b] In comparison, the Cp^*Ru^{II} and *p*-cymene Ru^{II} complexes bearing the significantly less bulky acetylacetone ligand feature a head-to-tail dimerization,

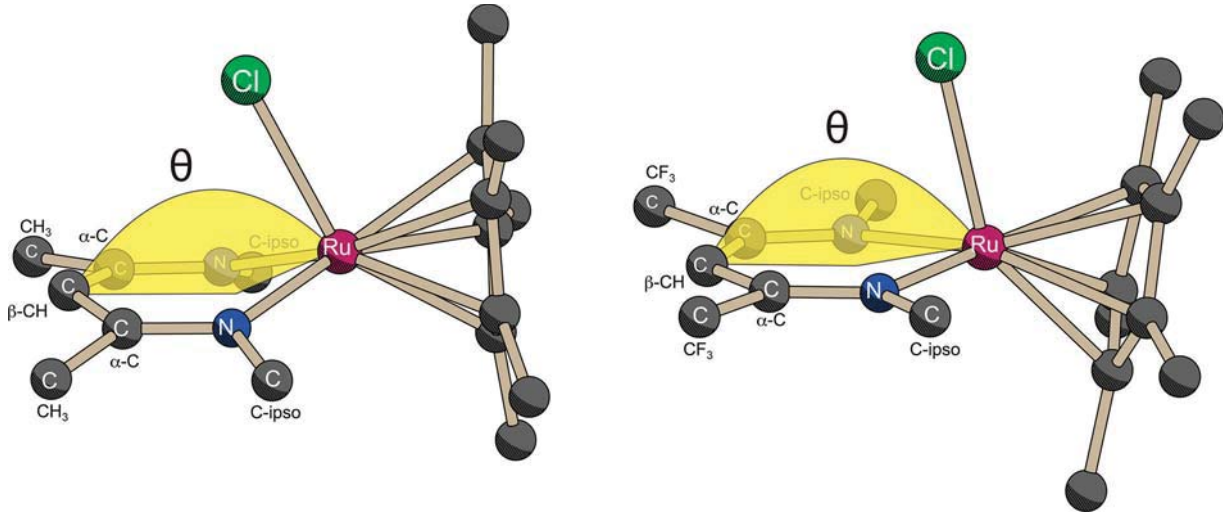

Figure 8. Comparison of the structure associated with the β-diketiminate ligands observed in the series of Ru^{III} complexes **7**−**11**: (left) envelope-type conformation found in **7** (R = CH_3, Ar = 2,6-dimethylphenyl) and **8** (R = CH_3, Ar = 3,5-dimethylphenyl), where θ = 154.6(1) and 166.3(2)°, respectively; (right) planar-type conformation found in **9** (R = CH_3, Ar = 3,5-bistrifluoromethylphenyl), **10** (R = CH_3, Ar = 3,5-dimethylphenyl), and **11** (R = CF_3, Ar = 3,5-bistrifluoromethylphenyl), where θ is equal to or greater than 171.6(2)°. In addition, **10** and **11** feature a second fold of the β-diketiminate ligand along the Ru···β-CH axis. The Cp*(centroid)−Ru−Cl bond angle remains constant throughout the entire series.

Table 4. Selected Bond Lengths (Å) and Angles (deg) for the Ru^{III} Complexes 7−11

	7	8	9[a]	10	11
Ru−N	2.075(2)	2.051(4)	2.067(12)	2.055(4)	2.071(3)
	2.089(2)	2.050(5)		2.069(4)	2.070(3)
$N-C_{ipso}$	1.452(4)	1.451(7)	1.432(17)	1.470(7)	1.443(4)
	1.453(4)	1.444(6)		1.452(7)	1.440(4)
$N-C_{\alpha}$	1.342(4)	1.332(7)	1.344(24)	1.331(6)	1.324(4)
	1.347(4)	1.329(7)		1.309(6)	1.329(4)
$C_{\alpha}-C_{\beta}$	1.402(5)	1.381(8)	1.387(23)	1.384(8)	1.390(5)
	1.399(5)	1.381(6)		1.394(7)	1.395(6)
Ru−Cl	2.461(1)	2.451(1)	2.437(2)	2.431(1)	2.430(1)
Ru−C[b]	1.890(1)	1.869(2)	1.868(6)	1.886(2)	1.881(2)
N−Ru−N	87.5(1)	87.8(2)	87.6(4)	90.2(2)	89.7(1)
$Ru-N-C_{ipso}$	120.8(2)	115.9(3)	116.3(10)	115.6(3)	115.4(2)
	119.7(2)	116.6(4)		116.8(3)	116.5(2)
$Ru-N-C_{\alpha}$	124.0(2)	127.6(3)	128.5(9)	125.7(3)	125.6(2)
	125.2(2)	126.4(4)		124.4(4)	125.7(2)
$N-C_{\alpha}-C_{\beta}$	123.7(3)	123.2(4)	123.3(14)	124.7(5)	125.5(4)
	123.5(3)	124.0(5)		126.0(5)	125.2(3)
$C_{\alpha}-C_{\beta}-C_{\alpha}$	127.4(3)	128.1(5)	128.8(13)	127.7(5)	127.6(3)
N−Ru−Cl	85.0(1)	87.7(1)	88.4(3)	86.7(1)	85.0(1)
	86.6(1)	86.2(1)		84.4(1)	85.7(1)
Cl−Ru−C[b]	115.6(1)	115.5(1)	115.6(2)	116.06(8)	114.4(6)
C[b]−Ru−N[c]	160.2(1)	158.8(1)	156.7(4)	160.25(14)	162.1(1)
Ru−N[c]−C_{β}	154.6(1)	166.3(2)	179.6(6)	171.6(2)	173.0(2)

[a]Four symmetry-independent molecules are found within the unit cell; the values reported are averaged. [b]Refers to the centroid point of the η^5-C_5Me_5 ligand. [c]Refers to the midpoint distance between the two nitrogen centers of the β-diketiminato ligand.

formed through bonding between the metal and β-C positions.[36] This particular binding mode is not observed in **13**−**17**. Therefore, the flanking aryl groups of β-diketiminate ligands are highly effective in sterically preventing the dimerization, which leads to stable complexes where the coordination number of ruthenium is reduced.

Only a limited number of structural changes to the β-diketiminate ligand were observed upon reduction of the Cl-binding Ru^{III} complexes, notably those parameters associated with the Ru−N bond distances and N−Ru−N bond angles. For example, the majority of Ru^{II} complexes feature shorter Ru−N bonds, except in the case of **9** (Ar = 3,5-$(CF_3)_2C_6H_3$), where the reduction from **9** to **15** leads to longer Ru−N bonds. The larger N−Ru−N bond angles associated with α-CF_3 substitution found in **10** and **11** are retained in the corresponding Ru^{II} species, **16** and **17**. In comparison, the metal−Cp*(centroid) distances are significantly shorter in the Ru^{II} complexes than in the corresponding Ru^{III} species, with the greatest change occurring on reduction of **8** to **14** (Ar = 3,5-$(CH_3)_2C_6H_3$). The shortened Cp*−Ru distances indicate

Table 5. Selected Bond Lengths (Å) and Angles (deg) for the Ru^{II} Complexes 13−17

	13	14	15	16	17[a]
Ru−N	2.071(2)	2.060(1)	2.040(5)	2.050(2)	2.055(6)
					2.056(6)
	2.060(3)	2.063(2)	2.046(4)	2.050(2)	2.035(6)
					2.025(6)
$N-C_{ipso}$	1.447(4)	1.446(2)	1.436(6)	1.457(3)	1.463(10)
					1.437(9)
	1.452(4)	1.447(2)	1.436(6)	1.454(3)	1.464(9)
					1.455(9)
$N-C_{\alpha}$	1.349(4)	1.347(2)	1.354(7)	1.346(3)	1.334(10)
					1.367(10)
	1.348(4)	1.345(2)	1.352(7)	1.344(3)	1.353(10)
					1.372(10)
$C_{\beta}-C_{\alpha}$	1.393(5)	1.398(3)	1.373(9)	1.391(3)	1.404(11)
					1.388(12)
	1.396(5)	1.398(3)	1.387(9)	1.394(3)	1.379(12)
					1.373(12)
Ru−C[b]	1.819(1)	1.809(1)	1.798(2)	1.824(1)	1.828(3)
					1.821(3)
N−Ru−N	87.2(1)	87.92(6)	87.4(2)	90.1(1)	89.6(3)
					89.3(2)
$Ru-N-C_{ipso}$	116.8(2)	115.92(11)	116.8(3)	116.8(1)	117.0(5)
					116.6(4)
	117.0(2)	116.02(11)	116.8(3)	116.2(1)	117.0(4)
					117.9(4)
$Ru-N-C_{\alpha}$	128.9(2)	128.46(12)	129.2(4)	126.2(1)	126.9(5)
					126.7(5)
	129.3(2)	128.64(12)	128.9(4)	126.3(1)	127.3(5)
					127.6(5)
$N-C_{\alpha}-C_{\beta}$	123.3(3)	123.48(16)	122.9(5)	125.1(2)	125.1(7)
					124.2(7)
	123.1(3)	123.27(17)	123.2(5)	125.0(2)	124.0(7)
					123.2(7)
$C_{\alpha}-C_{\beta}-C_{\alpha}$	128.1(3)	128.05(17)	128.2(5)	127.3(2)	127.4(7)
					128.6(7)
C[b]−Ru−N[c]	179.4(1)	179.7(1)	178.8(2)	179.8(1)	179.3(2)
					179.9(4)
Ru−N[c]−C_{β}	179.7(1)	176.8(1)	178.4(3)	178.9(1)	179.0(5)
					179.2(4)

[a]Two symmetry-independent molecules are found within the unit cell. [b]Refers to the centroid point of the η^5-C_5Me_5 ligand. [c]Refers to the midpoint distance between the two nitrogen centers of the β-diketiminato ligand.

increased metal−ligand interactions and are correlated with a more electron-rich β-diketiminato Ru^{II} fragment, donating into the π^* MOs associated with the Cp* ligand. A more detailed and comprehensive comparison of the metal−ligand interactions in the Ru^{III} and Ru^{II} complexes as analyzed through DFT-calculated models is discussed in the Supporting Information.

Interestingly, the shortened Ru^{II}−Cp*(centroid) distances are not correlated with the C_{ipso}−N-Ru bond angle, indicative of the steric interaction between the flanking aryl of the β-diketiminate ligand and the Cp* group. However, the 2,6-dimethyl aryl substitution in **13** leads to the five CH_3 groups of the Cp* being significantly distorted out of the ring plane, as indicated by an average Cp*(centroid)−C-C(Me) bond angle of 172.48°. In contrast, for complex **14**, which features a shorter Cp*-Ru interaction, the out-of-plane bending of the CH_3 substituents belonging to the Cp* are less than in **13**, where the average Cp*(centroid)−C-C(Me) bond angle is 173.51°, the greatest in the Ru^{II} series. Comparison of other bond parameters associated with the β-diketiminate ligand, particularly the $N-C_{\beta}$ and C_{β}-C_{α} bond distances, show little variation between oxidized **7** and reduced **13**.

Both sets of Ru^{II} and Ru^{III} complexes, incorporating β-diketiminate CF_3 groups, demonstrate crystal packing effects more complicated than those observed in the other complexes. In all cases involving CF_3 groups, the spatial packing involving complexes **9**−**11** and **15**−**17** maximizes the number of intermolecular fluorine−fluorine interactions, as observed in other organometallic complexes bearing fluorinated ligands[37] and organic molecules.[38] A more detailed discussion regarding intermolecular interactions is provided in the Supporting Information.

Electrochemical Analysis of Complexes 7−11 and 13−17. The redox properties of the Ru^{III} complexes **7**−**11** and Ru^{II} complexes **13**−**17** were characterized using cyclic and differential pulse voltammetry. Due to the propensity of the complexes toward bond activation, [*n*-Bu_4N]BArF was used as an inert supporting electrolyte in all measurements (Table 6).

Table 6. Electrochemical Data for 7−11 and 13−17[a]

complex	aryl	α-R	$E_{1/2}$ (V)	ΔE (mV)	E_{pc} (V)
7	2,6-$(CH_3)_2C_6H_3$	CH_3	0.39	331	−1.07
8	3,5-$(CH_3)_2C_6H_3$	CH_3	0.30	194	−0.23
9	3,5-$(CF_3)_2C_6H_3$	CH_3	0.56	359	−0.81
10	3,5-$(CH_3)_2C_6H_3$	CF_3	0.48[c,d]	170	−0.61
11	3,5-$(CF_3)_2C_6H_3$	CF_3	−0.25	332	−1.58[b]
13	2,6-$(CH_3)_2C_6H_3$	CH_3	0.36	394	
14	3,5-$(CH_3)_2C_6H_3$	CH_3	0.36	248	
15	3,5-$(CF_3)_2C_6H_3$	CH_3	0.16	189	
16	3,5-$(CH_3)_2C_6H_3$	CF_3	0.48	300	
17	3,5-$(CF_3)_2C_6H_3$	CF_3	0.05	229	−0.72, 0.57

[a]Conditions: in THF using [*n*-Bu_4N]BArF (0.026 M) as supporting electrolyte, potentials vs SCE referenced to external Fc^+/Fc ($E_{1/2}$ = 0.56 V), scan rate 250 mV s^{-1}. [b]Value from DPV. [c]Only observed after initial sample reduction. [d]A second reversible oxidation is observed: $E_{1/2}$ = 0.74 V, ΔE = 222 mV.

Complexes **13−17** showed quasi-reversible oxidations between +0.05 and +0.48 V. No clear correlation between the oxidation potentials and the electronic effect imparted by the substituents on the β-diketiminate was found. The electron-withdrawing CF_3 substituents tend to facilitate oxidation when located on the aryl ring, although they lead to a higher oxidation potential when positioned only within the β-diketiminato scaffold. Possibly, stereoelectronic effects may account for a more complex interplay between substituents and the metal center. Such effects may include charge delocalization within the six-membered β-diketiminato ruthenium unit entailing π back-bonding,[39] perhaps combined with a conformational rigidity of the aryl fragments that is dependent on the α-positioned substituents. The large variability of the oxidation potentials within the series suggests that the redox reaction is not a purely metal-centered process.

Compounds **7−11** display an irreversible reduction in addition to a quasi-reversible oxidation. While again no clear correlation is apparent, it is interesting to note that the redox process in **7**, **8**, and **10** are closely related to the electrochemical behavior of the corresponding analogues **13−15**, respectively (Figure 9). The irreversibility of the reduction implies a fast

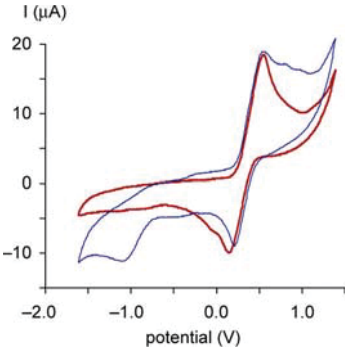

Figure 9. Superimposed graphs from cyclic voltammetric measurements of **7** (blue) and **13** (red), indicating the strong similarity of the oxidation around +0.38 V and the irreversible reduction of species **7** around −1 V.

chemical transformation following the reduction. It seems plausible that the electrochemically reduced complex 7^- rapidly undergoes chloride loss, thus forming **13**. Notably, **9** and **11**, both featuring CF_3 meta-substituted aryl groups, show a different behavior. In these complexes the reversible oxidation is not paralleled by a similar process when starting from the corresponding Ru^{II} analogues **15** and **17**, respectively, suggesting a more complicated electrochemically induced reaction sequence.

Evaluation of the Ru^{III} Complexes 7−11 in Atom Transfer Radical Addition Reactions. The atom transfer radical addition (ATRA) of polyhalogenated compounds to olefins ("Kharasch reaction")[40] is a versatile C−C coupling reaction with importance in organic synthesis.[41] In 1973 it was discovered that $Ru^{II}Cl_2(PPh_3)_3$ is a potent catalyst for this reaction.[42] Since then, several ruthenium complexes with high catalytic activity have been developed.[43] Among them are half-sandwich complexes with arene[44] and cyclopentadienyl ligands[45] and complexes bearing carborane,[46] amidinate,[32b,47] vinylidene,[48] alkylidene,[49] and N-heterocyclic carbene ligands,[50] as well as bimetallic complexes.[44b,51] Not surprisingly, the nature of the ligands is a decisive factor for the catalytic activity, and there is evidence that the ATRA activity correlates with the redox potential of the complexes.[52] Consequently, the catalytic activity of **7−11** in ATRA reactions was evaluated.

Ruthenium-catalyzed ATRA reactions are believed to proceed via a Ru^{II}/Ru^{III} redox couple, and Ru^{II} complexes are generally used as catalyst precursors.[43] Recently, however, it has been shown that Ru^{III} complexes can be used as the catalyst precursors if combined with AIBN[53] or Mg as a reducing agent.[51,54] The reducing agent generates and constantly regenerates the active Ru^{II} species. The use of Mg is particularly appealing, because it gives rise to low amounts of side products, and it can easily be separated from the reaction mixture and was thus chosen for the ATRA reactions with **7−11**.

The addition of CCl_4 to styrene, a commonly used benchmark reaction, was initially investigated.[43] All reactions were performed at room temperature with a substrate to catalyst ratio of 300:1. Since water-saturated solvents can be beneficial for ATRA reactions,[54d] all reactions were carried out in degassed "wet" deuterated toluene.

Complexes **7−11** were found to display very different catalytic activities (Table 7), and **7−9**, with a methyl substituent on the β-diketiminato ligand, were almost inactive, whereas **10** and **11**, which carry the electron-withdrawing CF_3 α-substituents, showed significantly higher activity. The highest yield of 76% was obtained with **11** as the catalyst (Table 7, entry 5).

Next, the ATRA of 4-toluenesulfonyl chloride (TsCl) to styrene was investigated.[55a] The reactions were carried out at room temperature using 1 mol % of the complexes, and the results are summarized in Table 8. The relative catalytic activities of the complexes differ from those observed for the reaction with CCl_4. The most active catalyst is **10**, leading to a yield of 87% (Table 8, entry 4), whereas **11**, which was the most active catalyst for CCl_4, displays only moderate activity in this reaction (Table 8, entry 5). However, the overall trend is similar, with complexes bearing electron-withdrawing CF_3 groups on the β-diketiminato ligand being more active.

Intramolecular ATRA reactions, often referred to as atom transfer radical cyclization (ATRC) reactions, are particularly interesting for organic synthesis, and several Cu and Ru complexes have successfully been employed as catalysts for this type of transformation.[41,43] The catalytic properties of species **7−11** in ATRC reactions were evaluated for the cyclization of *N*-allyl-*N*-phenyltrichloroacteamide (**A**)[47,b] and 2,2,2-trichloroethyl ether (**B**)[55] in the presence of Mg at room temperature. Using 5 mol % of catalyst, all Ru^{III} complexes showed some

Table 7. ATRA of CCl_4 to Styrene Catalyzed by 7−11 in the Presence of Mg[a]

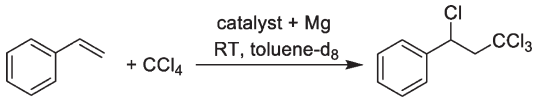

entry	cat-alyst	[catalyst]: [olefin]	conversion (%)	yield (%)
1	**7**	1:300	5	3
2	**8**	1:300	8	6
3	**9**	1:300	8	6
4	**10**	1:300	60	56
5	**11**	1:300	78	76

[a]Reactions were performed in the presence of activated Mg powder (100 mg) with D_2O-saturated toluene-d_8 as the solvent; [catalyst] = 4.6 mM, [styrene] = 1.38 M, [CCl_4] = 5.52 M, [internal standard] = 270 mM. The conversion is based on the consumption of the olefin, and the yield is based on the formation of the product determined by ^{1}H NMR spectroscopy using the internal standard 1,4-bis-(trifluoromethyl)benzene.

Table 8. ATRA of TsCl to Styrene Catalyzed by 7−11 in the Presence of Mg[a]

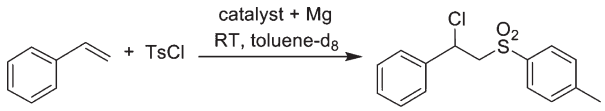

entry	cat-alyst	[catalyst]: [olefin]	conversion (%)	yield (%)
1	**7**	1:100	13	8
2	**8**	1:100	26	22
3	**9**	1:100	18	14
4	**10**	1:100	89	87
5	**11**	1:100	43	37

[a]Reactions were performed in the presence of activated Mg powder (100 mg) with D_2O-saturated toluene-d_8 as the solvent; [catalyst] = 4.4 mM, [styrene] = 0.44 M, [TsCl] = 0.52 M, [internal standard] = 90 mM. The conversion is based on the consumption of the olefin, and the yield is based on the formation of the product determined by ^{1}H NMR spectroscopy after 24 h using the internal standard 1,4-bis(trifluoromethyl)benzene.

level of activity, varying from moderate to very good (Table 9). For the cyclization of substrate **A**, complex **10** was the most active catalyst, leading to full conversion and a yield of 95% after only 5 h (Table 9, entry 4). For the cyclization of **3**, however, the best yields were observed with **7** (83%, Table 9, entry 6) and **9** (91%, Table 9, entry 8). The high activity of **7** and **9** is in sharp contrast to that observed for the ATRA reactions with CCl_4 (Table 1) and TsCl (Tables 7 and 8), in which **7** and **9** were not very active.

The results obtained for the different ATRA and ATRC reactions show that the complexes presented here, in combination with Mg, are potent catalysts for ATR-type reactions, leading to good yields under mild conditions. No simple correlation between catalytic activity and the redox potential of the complexes or the steric demand of the β-diketiminato ligand was observed. In contrast, complexes with a low activity for one reaction were found to be highly active for a different one. The strong dependence of the relative catalytic activity on the substrate parallels to some extent what has been observed for ruthenium based metathesis catalysts,[56] and should be considered for future investigations in this area.

Table 9. ATRC Reactions Catalyzed by 7−11 in the Presence of Mg[a]

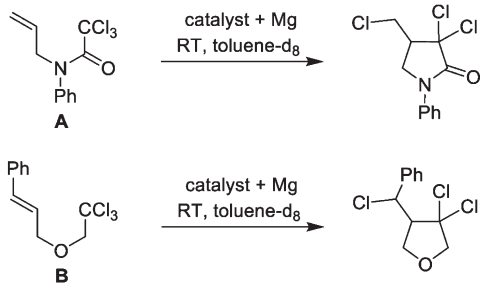

entry	substrate	cat-alyst	conversion (%)	yield (%)
1	**A**	**7**	57	54
2	**A**	**8**	62	60
3	**A**	**9**	47	45
4	**A**	**10**	100	95
5	**A**	**11**	81	76
6	**B**	**7**	90	83
7	**B**	**8**	37	35
8	**B**	**9**	98	91 (86:14)
9	**B**	**10**	63	57
10	**B**	**11**	10	7

[a]Reactions were performed in toluene-d_8 (total volume 1000 μL, [substrate] = 0.10 M, [Ru] = 5.0 mM). The conversion is based on the consumption of the olefin, and the yield is based on the formation of the product determined by ^{1}H NMR spectroscopy after 24 h using 1,4-bis(trifluoromethyl)benzene (50 mM) as the internal standard.

EXPERIMENTAL SECTION

General Procedures. Synthesis of the starting materials was carried out under a N_2 atmosphere with standard Schlenk techniques,[57] whereas subsequent preparations and manipulations, including catalytic reactions, were performed in a glovebox with a N_2 atmosphere, containing less than 1 ppm of O_2 and H_2O. Unless otherwise stated, all solvents were dried and degassed using appropriate scavenging columns (Innovative Technologies Inc.) and stored in Schlenk flasks equipped with Teflon stopcocks. Celite (541 grade, Aldrich) was dried at 180 °C before use. Benzene-d_6 and toluene-d_8 were dried over potassium and distilled under a N_2 atmosphere. Microwave reactions were performed using a Biotage initiator 2.0 reactor using metal-capped pressurized microwave vials. The protonated β-diketiminates **2**−**6**, the corresponding lithium complexes, and $[(\eta^5\text{-}C_5Me_5)Ru^{III}Cl_2]_2$ were prepared according to literature procedures.[24,58,59] Mg powder (>99%) was obtained from Fluka and was activated through agitation using a stirring bar under an atmosphere of dry N_2 for 10 days before use. All other reagents were purchased from commercial sources and used as received. NMR spectra were recorded on Bruker Avance instruments operating at 200 or 400 MHz. Where applicable, homo- and heteronuclear ^{1}H (COSY, NOE) and ^{13}C (HMBC and HSQC) NMR correlation spectroscopy was used to assign molecular connectivity. Chemical shifts for ^{1}H and ^{13}C spectra were referenced with respect to the ^{1}H or ^{13}C signal of residual nondeuterated solvents in the sample, and ^{19}F spectra were referenced to CF_3Cl. All NMR samples were prepared under a N_2 atmosphere and stored in flame-sealed glass NMR tubes. Attenuated transmitted reflectance FT-IR spectra were acquired on a Perkin-Elmer Spectrum-One instrument with diamond-anvil configuration, or for air-sensitive complexes, Nujol mull suspensions were kept between KBr plates placed in a gasket-sealed sample holder. Elemental analyses were obtained using an Exeter Analytical CE-440 elemental analyzer. Suitable elemental analyses for complexes **11**−**17** could not be obtained, due to their high sensitivity to oxygen. Mass spectra were recorded using ESI-MS under standard conditions employed for organometallic compounds[60] on a Thermo-Finnigan LCQ DECA XP

Plus quadruple ion trap instrument set in positive mode: flow rate 5 μL per min; spray voltage 5 kV; capillary temperature 100 °C; capillary voltage 20 V. UV−visible absorption spectra were recorded using diluted stock solutions of *n*-pentane or CH_2Cl_2 and measured in Teflon cap sealed quartz Suprasil cuvette (1 cm path length) on a Jasco V-550 spectrometer at 25 °C. Electrochemical studies were carried out using an EG&G Princeton Applied Research Model 273A potentiostat employing a gas tight three-electrode cell under an argon atmosphere. A saturated calomel electrode (SCE) was used as reference; a Pt disk (3.14 mm^2) and a Pt wire were used as the working and counter electrodes, respectively. The redox potentials were measured in THF (~1 mM) with *n*-$Bu_4N(BArF)$ (0.026 M) as the supporting electrolyte and ferrocene ($E_{1/2}$ = 0.56 V vs SCE) as an external standard. Crystallographic details and data tables are provided in the Supporting Information.

Synthesis of (η^5-$C_5(CH_3)_5$)Ru(Cl)(2,6-$(CH_3)_2C_6H_3NC(CH_3))_2CH$ (7). Li[(2,6-$(CH_3)_2C_6H_3NC(CH_3))_2CH$] (**2-Li**; 0.254 g, 0.813 mmol) was dissolved in CH_2Cl_2 (5 mL). This solution was added dropwise to $[(\eta^5\text{-}C_5(CH_3)_5)RuCl_2]_2$ (0.250 g, 0.410 mmol) dissolved in CH_2Cl_2 (5 mL). This mixture was stirred for 8 h and then filtered through Celite. The solvent volume was reduced under vacuum, and 25 mL of *n*-pentane was added to precipitate a blue solid that was filtered and washed with 3 × 10 mL of *n*-pentane. Further purification involved dissolving the crude complex in 25 mL of Et_2O and filtering through Celite. The solvent was removed under reduced pressure, and the resulting solid was dried under high vacuum for 24 h. Yield: 84% (0.389 g). Single crystals suitable for structural analysis by X-ray diffraction were grown by slow diffusion of *n*-pentane into a saturated CH_2Cl_2 solution containing **7**.

Anal. Found (calcd): C, 63.80 (64.51); H, 7.08 (6.99); N, 4.67 (4.85). FT-IR (25 °C, solid; ν (cm^{-1})): 3071 (w); 2921 (w); 1590 (w); 1537 (m); 1507 (w); 1416 (m); 1432 (m); 1371 (m); 1346 (s); 1278 (m); 1266 (m); 1209 (m); 1186 (m); 1161 (w); 1096 (w); 1073 (w); 1018 (m); 986 (w); 919 (w); 849 (m); 812 (m); 769 (s); 705 (w). ESI-MS (positive mode; *m*/*z*): 543.3 [$M^+ - Cl^-$]. UV−visible (25 °C, CH_2Cl_2; λ (nm) [ε (cm^{-1} L mol^{-1})]): 646 [4428], 318 [20 328].

Synthesis of (η^5-$C_5(CH_3)_5$)Ru(Cl)(3,5-$(CH_3)_2C_6H_3NC(CH_3))_2CH$ (8). The procedure is identical with that employed for **7**, using the following quantities: 0.254 g of Li[(3,5-$(CH_3)_2C_6H_3NC(CH_3))_2CH$] (**3-Li**; 0.813 mmol), with 0.250 g of $[(\eta^5\text{-}C_5(CH_3)_5)RuCl_2]_2$ (0.407 mmol). Yield: 59% (0.275 g), light blue complex. Anal. Found (calcd): C, 64.52 (64.51); H, 7.31 (6.99); N, 4.62 (4.85). FT-IR (25 °C, solid; ν (cm^{-1})): 2898 (w); 1599 (w); 1587 (m); 1541 (m); 1511 (w); 1442 (w, br); 1369 (w); 1346 (s); 1308 (w); 1286 (w); 1276 (w); 1161 (w); 1149 (w); 1115 (w, br); 1072 (w); 1027 (m); 912 (w); 848 (m); 792 (m); 758 (w); 693 (m). ESI-MS (positive mode; *m*/*z*): 543.3 [$M^+ - Cl^-$]. UV−visible (25 °C, CH_2Cl_2; λ (nm) [ε (cm^{-1} L mol^{-1})]): 637 [5535], 318 [27 621].

Synthesis of (η^5-$C_5(CH_3)_5$)Ru(Cl)(3,5-$(CF_3)_2C_6H_3NC(CH_3))_2CH$ (9). The procedure is identical with that employed for **7**, using the following quantities: 0.425 g of Li[(3,5-$(CF_3)_2C_6H_3NC(CH_3))_2CH$] (**4-Li**; 0.805 mmol), with 0.250 g of $[(\eta^5\text{-}C_5(CH_3)_5)RuCl_2]_2$ (0.407 mmol). Yield: 72% (0.582 g), light blue solid. Anal. Found (calcd): C, 46.95 (46.61); H, 3.56 (3.57); N, 3.48 (3.53). FT-IR (25 °C, solid); ν (cm^{-1})): 1543 (w); 1517 (w); 1465 (w); 1433 (w); 1373 (m); 1348 (m); 1277 (s); 1262 (w); 1196 (m); 1173 (m); 1127 (s); 1105 (m); 1069 (w); 1037 (w); 1019 (w); 983 (m); 931 (w); 921 (w); 899 (m); 885 (w); 847 (m); 805 (w); 718 (m); 705 (w); 682 (s). ESI-MS (positive mode; *m*/*z*): 759.4 [$M^+ - Cl^- + H^+$]. UV−visible (25 °C, CH_2Cl_2; λ (nm) [ε (cm^{-1} L mol^{-1})]): 636 [5067], 322 [28 512].

Synthesis of (η^5-$C_5(CH_3)_5$)Ru(Cl)(3,5-$(CH_3)_2C_6H_3NC(CF_3))_2CH$ (10). The procedure is identical with that employed for **7**, using the following quantities: 0.176 g of Li[(3,5-$(CH_3)_2C_6H_3NC(CF_3))_2CH$] (**5-Li**; 0.419 mmol), in 10 mL of CH_2Cl_2 with 0.250 g of $[(\eta^5\text{-}C_5(CH_3)_5)RuCl_2]_2$ (0.407 mmol) in 12 mL of CH_2Cl_2. Yield: 58% (0.287 g), pale green microcrystalline solid. Anal. Found (calcd): C, 54.54 (54.35); H, 5.35 (5.00); N, 3.89 (4.09). FT-IR (25 °C, solid; ν (cm^{-1})): 1619 (w); 1567 (w); 1485 (w); 1471 (w); 1415 (w); 1366 (s); 1309 (w); 1283 (s); 1276 (s); 1218 (m); 1175 (s); 1165 (s); 1132 (s); 1112 (s); 1106 (s); 1017 (w); 1004 (w); 964 (m); 903 (w); 903 (m); 846 (m); 809 (w); 785 (w); 723 (m); 713 (m); 682 (s). ESI-MS (positive mode; *m*/*z*): 651.3 [$M^+ - Cl^- + H^+$]. UV−visible (25 °C, CH_2Cl_2; λ (nm) [ε (cm^{-1} L mol^{-1})]): 606 [3954], 410 [8209], 349 [26 790].

Synthesis of (η^5-$C_5(CH_3)_5$)Ru(Cl)(3,5-$(CF_3)_2C_6H_3NC(CF_3))_2CH$ (11). *Method A.* This procedure is identical with that employed for **7**, using the following quantities: 0.522 g of Li[(3,5-$(CF_3)_2C_6H_3NC(CF_3))_2CH$] (**6-Li**; 0.820 mmol), in 30 mL of CH_2Cl_2 with 0.250 g of $[(\eta^5\text{-}C_5(CH_3)_5)RuCl_2]_2$ (0.407 mmol) in 2.5 mL of CH_2Cl_2. Yield: 60% (0.357 g).

Method B. The β-diketiminato silver precursor [Ag(3,5-$(CF_3)_2C_6H_3NC(CF_3))_2CH)(MeCN)_2]_2$ (**18**) was prepared by adding (3,5-$(CF_3)_2C_6H_3NC(CF_3))_2CH_2$ (**6-H**; 0.394 g, 0.629 mmol) to Ag_2O (0.150 g, 0.647 mmol) in 40 mL of degassed wet acetonitrile. This solution was heated using a microwave reactor at 400 MW for 1 h. The resulting red solution was filtered under N_2 through a 1 cm pad of Celite and the solvent removed under vacuum. The obtained brown-yellow powder was washed with *n*-pentane and dried under vacuum, protected from light. The final yield was 89% (0.432 g). Spectroscopic data of the complex [Ag(3,5-$(CF_3)_2C_6H_3NC(CF_3))_2CH)(MeCN)_2]_2$ (**18**) are identical with those reported in the literature.[14a]

A 0.255 g portion of [Ag(3,5-$(CF_3)_2C_6H_3NC(CF_3))_2CH)(MeCN)_2]_2$ (**18**) was dissolved in 50 mL of CH_2Cl_2, and this solution was added dropwise to a solution of $[(\eta^5\text{-}C_5(CH_3)_5)RuCl_2]_2$ (0.101 g, 0.163 mmol) in 10 mL of CH_2Cl_2 over a period of 20 min. The reaction mixture was stirred for 16 h with exclusion of light, after which a mixture of a dark green solution and white-gray precipitate was obtained. The solution was filtered through a 1 cm pad of Celite and the solvent removed using vacuum. The dark green solid was washed with 125 mL of *n*-pentane and then 75 mL of Et_2O. Further purification involved dissolving the crude complex in a minimal amount of CH_2Cl_2 (5 mL) and reprecipitating using 50 mL of *n*-pentane. The resulting solid was collected, washed with 3 × 10 mL of *n*-pentane, and dried under vacuum to afford complex **11** in 68% yield (0.100 g).

Method C. A solution of (3,5-$(CF_3)_2C_6H_3NC(CF_3))_2CH_2$) (**6-H**; 0.250 g, 0.397 mmol) dissolved in 30 mL of THF was combined with TlOEt (0.109 g, 0.436 mmol), causing an instantaneous color change from yellow to deep orange. The reaction mixture was stirred for 2 h with the exclusion of light. Afterward, the solvent was removed under vacuum, resulting in an orange solid. ^1H, ^{13}C, and ^{19}F NMR data for Tl(3,5-$(CF_3)_2C_6H_3NC(CF_3))_2CH$) (**19**) are given below.

^1H NMR (30 °C, 399.8 MHz, C_6D_6; δ (ppm)): 0.94 (t, $^2J_{HH}$ = 7 Hz, 3H, CH_3CH_2OH), 3.35 (q, $^2J_{HH}$ = 7 Hz, 2H, CH_3CH_2OH), 5.89 (s, 1H, β-*CH*), 7.21 (s, 4H, Ar *o*-*CH*), 7.58 (s, 2H, Ar *p*-*CH*). ^{13}C NMR (30 °C, 100.5 MHz, C_6D_6; δ (ppm)): 19.2 (s, CH_3CH_2OH), 58.4 (s, CH_3CH_2OH), 90.9 (m, β-*C*H), 117.8 (sept, $^3J_{CF}$ = 3.8 Hz, *p*-*C*H), 121.8 (q, $^1J_{CF}$ = 289.1 Hz, α-CF_3), 122.9 (s, *o*-CCH_3), 124.0 (q, $^1J_{CF}$ = 273.0 Hz, *m*-CF_3), 133.4 (q, $^2J_{CF}$ = 33.3 Hz, Ar *m*-CCF_3), 151.2 (s, Ar i-*C*), 151.4 (q, $^1J_{CF}$ = 25.9 Hz, α-CF_3C). ^{19}F NMR (30 °C, 376.1 MHz, C_6D_6; δ (ppm)): −62.79 (s, 12F, *m*-CF_3), −60.23 (s, 6F, α-CF_3).

Complex **19** was dissolved in 30 mL of CH_2Cl_2 and added dropwise to a solution of $[(\eta^5\text{-}C_5(CH_3)_5)RuCl_2]_2$ (0.122 g, 0.198 mmol) in 25 mL of CH_2Cl_2. The solution was stirred for 14 h with exclusion of light. Afterward the reaction mixture was filtered through a 1 cm pad of Celite and the solvent removed using vacuum. The residue was washed with 125 mL of *n*-pentane and then 75 mL of Et_2O. The product was purified by dissolving the crude complex in a minimal amount of CH_2Cl_2 (10 mL) and precipitated with 150 mL of *n*-pentane. The resulting solid was collected on a frit, washed with 3 × 10 mL of *n*-pentane, and dried under vacuum, to afford complex **11** (0.301 g) in 84% yield.

Single crystals suitable for structural analysis by X-ray diffraction were grown by slow diffusion of *n*-pentane into a saturated CH_2Cl_2 solution of **11** kept at 4 °C.

Anal. Found (calcd): C, 42.07 (41.32); H, 2.82 (2.46); N, 3.01 (3.11). FT-IR (25 °C, solid; ν (cm^{-1})): 3004 (w); 2909 (w); 1605 (w); 1592 (w); 1559 (w); 1527 (w); 1483 (w); 1446 (w); 1417 (m);

1382 (w); 1374 (w); 1352 (w); 1313 (m); 1293 (m, sh); 1278 (w); 1260 (w); 1208 (m); 1187 (s); 1156 (s); 1130 (s); 1108 (m); 1072 (w); 1026 (m); 999 (w); 972 (w); 955 (w); 863 (w); 853 (m); 796 (m); 766 (w); 715 (m); 704 (m); 699 (m). ESI-MS (positive mode; m/z): 867.2 [$M^+ - Cl^- + H^+$]. UV−visible (25 °C, CH_2Cl_2; λ (nm) [ε (cm^{-1} L mol^{-1})]): 586 [3532], 420 [9552], 345 [24 675].

Synthesis of (η^5-$C_5(CH_3)_5$Ru(2,6-$(CH_3)_2C_6H_3NC(CH_3)$)$_2$CH (13). (η^5-$C_5(CH_3)_5$RuCl(2,6-$(CH_3)_2C_6H_3NC(CH_3)$)$_2$CH) (**7**; 0.327 g, 0.567 mmol) was dissolved in THF (10 mL). To this solution was added activated zinc filings (0.108 g, 1.65 mmol, approximately 3 mol excess) directly to the flask, and the mixture was stirred for 14 h. Gradually the solution changed from dark blue to dark red. Afterward, the solvent was removed using vacuum and the residue was extracted with 40 mL of *n*-pentane and passed through Celite. The solvent was removed using vacuum, affording a magenta solid, which was dried under vacuum for 10 h. Yield: 89.3% (0.274 g). ^{1}H NMR (25 °C, 400 MHz, C_6D_6; δ (ppm)): 0.938 (s, 15H, η^5-$C_5(CH_3)_5$), 1.734 (s, 6H, α-CH_3), 2.187 (s, 12H, Ar *o*-CH_3), 5.455 (s, 1H, β-*CH*), 7.066 (t, $^3J_{HH}$ = 7.32 Hz, 2H, Ar *p*-*CH*), 7.212 (t, $^3J_{HH}$ = 7.32 Hz, 4H, Ar *m*-*CH*). ^{13}C NMR (25 °C, 101 MHz, C_6D_6; δ (ppm)): 9.982 (s, η^5-$C_5(CH_3)_5$), 19.78 (s, α-CH_3), 23.93 (s, Ar *o*-CH_3), 77.16 (s, η^5-$C_5(CH_3)_5$), 98.86 (s, β-CH), 124.39 (s, Ar *p*-CH), 132.14 (s, Ar *m*-CH), 131.58 (s, Ar *o*-*C*), 157.53 (s, α-CCH_3), 157.854 (s, Ar *i*-*C*). FT-IR (25 °C, Nujol mull, KBr disks; ν (cm^{-1})): 1546 (s); 1509 (m); 1283 (w); 1263 (m); 1239 (w); 1214 (w); 1191 (m); 1160 (m); 1089 (w); 1072 (w); 1029 (m); 1018 (m); 984 (w); 846 (w); 786 (w); 763 (s); 722 (w); 709 (w). UV−visible (25 °C, *n*-pentane; λ (nm) [ε (cm^{-1} L mol^{-1})]): 306 [40 26].

Synthesis of (η^5-$C_5(CH_3)_5$)Ru(3,5-$(CH_3)_2C_6H_3NC(CH_3)$)$_2$CH (14). The procedure is identical with that employed for **13**, except the following quantities were used: 0.278 g of (η^5-$C_5(CH_3)_5$RuCl(3,5-$(CH_3)_2C_6H_3NC(CH_3)$)$_2$CH) (**8**; 0.482 mmol), in 15 mL of THF with 0.182 g of Zn (2.78 mmol). Yield: 87% (0.226 g), magenta solid. Single crystals suitable for structural analysis by X-ray diffraction were grown by slow evaporation of a saturated *n*-pentane solution containing **14**. ^{1}H NMR (25 °C, 400 MHz, C_6D_6; δ (ppm)): 1.243 (s, 15H, η^5-$C_5(CH_3)_5$); 2.136 (s, 6H, α-CH_3); 2.377 (s, 12H, Ar *m*-CH_3); 5.553 (s, 1H, β-*CH*); 6.844 (s, 2H, Ar *p*-*CH*); 7.030 (s, 4H, Ar *o*-*CH*). ^{13}C NMR (25 °C, 101 MHz, C_6D_6; δ (ppm)): 10.03 (s, η^5-$C_5(CH_3)_5$); 21.23 (s, Ar *m*-CH_3); 24.91 (s, α-CH_3), 77.74 (s, η^5-$C_5(CH_3)_5$); 98.13 (s, β-*CH*); 123.71 (s, Ar *o*-*CH*), 125.22 (s, Ar *p*-*CH*); 137.42 (s, Ar *m*-CCH_3); 157.36 (s, α-CCH_3); 159.66 (s, Ar *i*-*C*). FT-IR (25 °C, Nujol mull, KBr disks; ν (cm^{-1})): 1604 (m); 1589 (m); 1541 (s); 1507 (m); 1457 (s); 1366 (s); 1307 (m); 1278 (m); 1161 (w); 1146 (m); 1070 (w); 1028(m br.); 998 (w); 947 (w); 901 (w); 880 (w); 845 (m); 851 (m); 767 (w); 759 (w); 692 (m); 600 (w); 589 (w); 571 (w); 546 (w). UV−visible (25 °C, *n*-pentane; λ (nm) [ε (cm^{-1} L mol^{-1})]): 308 [50 199].

Synthesis of (η^5-$C_5(CH_3)_5$)Ru(3,5-$(CF_3)_2C_6H_3NC(CH_3)$)$_2$CH (15). The procedure is identical with that employed for **13**, except the following quantities were used: 0.360 g of (η^5-$C_5(CH_3)_5$RuCl(3,5-$(CF_3)_2C_6H_3NC(CH_3)$)$_2$CH) (**9**; 0.454 mmol), in 35 mL of THF with 0.125 g of Zn (1.91 mmol). Yield: 92% (0.317 g), magenta solid. Single crystals suitable for structural analysis by X-ray diffraction were grown by slow evaporation of a saturated benzene solution containing **13**. ^{1}H NMR (25 °C, 400 MHz, C_6D_6; δ (ppm)): 0.864 (s, 15H, η^5-$C_5(CH_3)_5$); 1.632 (s, α-CH_3); 5.294 (s, 1H, α-*CH*); 7.651 (s, 4H, Ar *o*-*CH*); 7.806 (s, 2H, Ar *p*-*CH*). ^{13}C NMR (25 °C, 101 MHz, C_6D_6; δ (ppm)): 9.67 (s, η^5-$C_5(CH_3)_5$); 25.20 (s, Ar *o*-CH_3); 78.15 (s, η^5-$C_5(CH_3)_5$); 99.28 (s, β-*CH*); 117.35 (q, $^3J_{CF}$ = 3.9 Hz, Ar *p*-CH); 123.87 (q, $^1J_{CF}$ = 272 Hz, Ar *m*-CCF_3); 125.55 (q, $^3J_{CF}$ = 2.7 Hz, Ar *o*-CH); 131.87 (q, $^2J_{CF}$ = 35 Hz, *m*-CCF_3); 157.97 (s, α-CCH_3); 159.58 (s, Ar *i*-*C*). ^{19}F NMR (25 °C, 181 MHz, C_6D_6; δ (ppm)): −62.91 (s, $^1J_{FC}$ = 272 Hz, Ar *m*-CF_3). FT-IR (25 °C, Nujol mull, KBr disks; ν (cm^{-1})): 1618 (w); 1605 (w); 1547 (m); 1512 (m); 1436 (m); 1431 (m); 1276 (s); 1220 (w); 1169 (s); 1126 (s); 1104 (m); 1092 (w); 1059 (m); 1023 (m); 1003 (w); 983 (m); 917 (m); 891 (s); 872 (w); 847 (m); 783 (w); 767 (w); 760 (w); 718 (m); 704 (m); 683 (s). UV−visible (25 °C, *n*-pentane; λ (nm) [ε (cm^{-1} L mol^{-1})]): 387 [6300], 314 [53 019].

Synthesis of (η^5-$C_5(CH_3)_5$)Ru(3,5-$(CH_3)_2C_6H_3NC(CF_3)$)$_2$CH (16). The procedure is identical with that employed for **13**, except the following quantities were used: 0.313 g of (η^5-$C_5(CH_3)_5$RuCl(3,5-$(CH_3)_2C_6H_3NC(CF_3)$)$_2$CH) (**10**; 0.457 mmol), in 20 mL of THF with 0.172 g of Zn (2.63 mmol). The reaction mixture was stirred for 14 h. Yield: 84% (0.297 g), red solid. Single crystals suitable for structural analysis by X-ray diffraction were grown by slow evaporation of saturated benzene solution containing **16**. ^{1}H NMR (25 °C, 400 MHz, C_6D_6; δ (ppm)): 0.973 (s, 15H, η^5-$C_5(CH_3)_5$); 2.340 (s, 12H, Ar *m*-CH_3); 6.819 (s, 2H, Ar *p*-*CH*); 7.080 (s, 1H, β-*CH*); 7.143 (s, 4H, Ar *o*-*CH*). ^{13}C NMR (25 °C, 101 MHz, C_6D_6; δ (ppm)): 9.25 (s, η^5-$C_5(CH_3)_5$); 20.95 (s, Ar *m*-CH_3); 83.42 (s, η^5-$C_5(CH_3)_5$); 90.24 (s, β-*CH*); 123.05 (q, $^1J_{CF}$ = 295 Hz, α-CCF_3); 123.88 (s, Ar *o*-CH); 126.74 (s, Ar *p*-CH); 136.34 (s, Ar *m*-CCH_3); 145.78 (q, $^2J_{CF}$ = 25 Hz, α-CCF_3); 155.81 (s, Ar *i*-*C*). ^{19}F NMR (25 °C, 181 MHz, C_6D_6; δ (ppm)): −55.97 (s, $^1J_{FC}$ = 295 Hz, α-CCF_3). FT-IR (25 °C, Nujol mull, KBr disks; ν (cm^{-1})): 1626 (w); 1605 (w); 1592 (m); 1565 (m); 1430 (s); 1309 (s); 1289 (m); 1272 (m), 1201 (s); 1167 (s); 1148 (s); 1136 (s); 1105 (m); 1074 (w); 1026 (m); 859 (w); 849 (m); 813 (m); 809 (w); 713 (m); 559 (w); 474 (w). UV−visible (25 °C, *n*-pentane; λ (nm) [ε (cm^{-1} L mol^{-1})]): 447 [7669], 317 [33 984].

Synthesis of (η^5-$C_5(CH_3)_5$)Ru(3,5-$(CF_3)_2C_6H_3NC(CF_3)$)$_2$CH (17). The procedure is identical with that employed for complex **13**, except the following quantities were used: 0.295 g of (η^5-$(C_5(CH_3)_5)$RuCl(3,5-$(CF_3)_2C_6H_3NC(CF_3)$)$_2$CH) (**11**; 0.327 mmol), in 15 mL of THF with 0.152 g of Zn (2.32 mmol). Yield: 91.3% (0.259 g), red solid. Single crystals suitable for X-ray diffraction were grown by slow evaporation of a saturated benzene solution of **17**. ^{1}H NMR (25 °C, 400 MHz, C_6D_6); δ (ppm)): 0.476 (s, 15H, η^5-$C_5(CH_3)_5$); 6.714 (s, 1H, β-*CH*); 7.681 (s, 2H, Ar *p*-*CH*); 7.684 (s, 4H, Ar *o*-*CH*). ^{13}C NMR (25 °C, 101 MHz, C_6D_6; δ (ppm)): 8.81 (s, η^5-$C_5(CH_3)_5$); 84.39 (s, η^5-$C_5(CH_3)_5$); 91.33 (s, β-CH); 119.00 (s, Ar *p*-CH); 122.27 (q, $^1J_{CF}$ = 271 Hz, α-CCF_3); 123.74 (q, $^1J_{CF}$ = 324 Hz, Ar m-CCF_3); 126.00 (s, Ar *o*-CH); 130.91 (q, $^2J_{CF}$ = 33 Hz, Ar *m*-CCF_3); 146.27 (q, $^2J_{CF}$ = 25 Hz, α-CCF_3); 155.65 (s, Ar *i*-*C*). ^{19}F NMR (25 °C, 181 MHz, C_6D_6; δ (ppm)): −56.59 (s, $^1J_{FC}$ = 271 Hz, α-CF_3); −63.05 (s, $^1J_{FC}$ = 324 Hz, Ar *m*-CF_3). FT-IR (25 °C, Nujol mull, KBr disks; ν (cm^{-1})): 1634 (w); 1620 (w); 1611 (w); 1567 (m); 1424 (m); 1308 (s); 1278 (s); 1247 (s); 1221 (s); 1127 (s); 1023 (m); 1003 (w); 984 (w); 966 (s); 918 (w); 918 (w); 901 (m); 897 (m); 891 (m); 847 (m); 817 (m); 804 (w); 722 (s); 710 (s); 683 (s); 582 (w); 539 (w); 476 (w). UV−visible (25 °C, *n*-pentane; λ (nm) [ε (cm^{-1} L mol^{-1})]): 448 [8481], 318 [36 035].

General Procedures for the Catalytic ATRA and ATRC Reactions. An aliquot of a stock solution containing the appropriate catalyst **7**−**11** in toluene-d_8 was added to a 1.5 mL vial containing Mg powder (100 mg). This mixture was stirred for 10 min. A stock solution of substrate was prepared in the following manner: D_2O (20 μL) was added to a freshly prepared toluene-d_8 solution containing the substrate (CCl_4, TsCl, **A** or **B**), styrene (only for ATRA reactions), and an internal standard, 1,4-bis(trifluoromethyl)-benzene. This mixture was shaken for 1 min to saturate the solution with D_2O. An aliquot of this stock solution was added to the reaction vial, and the total volume was completed to 1000 μL with toluene-d_8. After the mixture was stirred for 24 h at 25 °C, a sample (ATRA, 20 μL; ARTC, 40 μL) was removed from the reaction mixture, diluted with $CDCl_3$ (500 μL), and analyzed by ^{1}H NMR spectroscopy. Table 10 details the concentration of each reagent in the reactions.

Table 10. Concentration of the Components Used in the ATRA and ATRC Reactions

reaction type	substrate	[cat.] (mM)	[substrate] (M)	[styrene] (M)	[internal std] (mM)
ATRA	CCl_4	4.6	5.52	1.38	270
ATRA	TsCl	4.4	0.52	0.44	90
ATRC	**A** or **B**	5.0	0.10	n/a	50

■ ASSOCIATED CONTENT

Supporting Information

Computational analysis describing electronic molecular orbital structure and simulation of UV−visible spectra with band assignment for complexes **7**, **11**, **13**, and **17**. A detailed discussion regarding the solid-state packing. Experimental details for the crystallographic analysis of complexes **7**−**17**. The accompanying CIF contains additional crystallographic data. This material is available free of charge via the Internet at http://pubs.acs.org.

■ AUTHOR INFORMATION

Corresponding Author

*E-mail: paul.dyson@epfl.ch.

■ ACKNOWLEDGMENTS

This research was supported by grants from the European Commission Marie Curie Action (ADP, MEIF-CT-2005-025287, *CARCAS*), the Swiss National Science Foundation, the Ecole Polytechnique Fédérale de Lausanne, and University College Dublin. A.D.P. thanks the Science Foundation Ireland (SFI) for a Stokes Lectureship at UCD.

■ REFERENCES

(1) (a) Grubbs, R. H. Introduction. In *Handbook of Metathesis*; Grubbs, R. H., Ed. Wiley-VCH: Weinheim, Germany, 2003; Vol. *1*, pp 1−3. (b) Trnka, T. M.; Grubbs, R. H. *Acc. Chem. Res.* **2000**, *34*, 18−29.

(2) (a) Kakiuchi, F. *J. Synth. Org. Chem.* **2004**, *62*, 14−26. (b) Kakiuchi, F.; Murai, S. *Acc. Chem. Res.* **2002**, *35*, 826−834.

(3) Kitamura, M.; Noyori, R. Hydrogenation and Transfer Hydrogenation. In *Ruthenium in Organic Synthesis*; Murahasi, S.-I., Ed.; Wiley-VCH: Weinheim, Germany, 2004; pp 3−52.

(4) (a) Naota, T.; Takaya, H.; Murahashi, S. I. *Chem. Rev.* **1998**, *98*, 2599−2660. (b) Griffith, W. P. *Ruthenium Oxidation Complexes; Their Uses as Homogenous Organic Catalysts*; Springer: Heidelberg, Germany, 2011; Vol. *34*. (c) Murahashi, S.-I.; Komiya, N. Ruthenium-catalyzed Oxidation of Alkenes, Alcohols, Amines, Amides, beta-Lactams, Phenols, and Hydrocarbons. In *Modern Oxidation Methods*; Bäckvall, J.-E., Ed.; Wiley-VCH: Weinheim, Germany, 2004; pp 165−192.

(5) Mohamed, A. A. *Coord. Chem. Rev.* **2010**, *254*, 1918−1947.

(6) (a) Kitamura, M.; Hsiao, Y.; Noyori, R.; Takaya, H. *Tetrahedron Lett.* **1987**, *28*, 4829−4832. (b) Ikariya, T.; Murata, K.; Noyori, R. *Org. Biomol. Chem.* **2006**, *4*, 393−406.

(7) Edelmann, F. T. *Adv. Organomet. Chem.* **2008**, *57*, 183−352.

(8) Bourget-Merle, L.; Lappert, M. F.; Severn, J. R. *Chem. Rev.* **2002**, *102*, 3031−3065.

(9) (a) Hardman, N. J.; Eichler, B. E.; Power, P. P. *Chem. Commun.* **2000**, 1991−1992. (b) Cui, C. M.; Roesky, H. W.; Schmidt, H. G.; Noltemeyer, M.; Hao, H. J.; Cimpoesu, F. *Angew. Chem., Int. Ed.* **2000**, *39*, 4274−4276. (c) Driess, M.; Yao, S. H.; Brym, M.; van Wullen, C. *Angew. Chem., Int. Ed.* **2006**, *45*, 6730−6733. (d) Hill, M. S.; Hitchcock, P. B.; Pongtavornpinyo, R. *Angew. Chem., Int. Ed.* **2005**, *44*, 4231−4235.

(10) (a) Holland, P. L. *Acc. Chem. Res.* **2008**, *41*, 905−914. (b) Chai, J. F.; Zhu, H. P.; Stuckl, A. C.; Roesky, H. W.; Magull, J.; Bencini, A.; Caneschi, A.; Gatteschi, D. *J. Am. Chem. Soc.* **2005**, *127*, 9201−9206. (c) Cramer, C. J.; Tolman, W. B. *Acc. Chem. Res.* **2007**, *40*, 601−608. (d) Hayes, P. G.; Piers, W. E.; McDonald, R. *J. Am. Chem. Soc.* **2002**, *124*, 2132−2133. (e) Mindiola, D. J. *Angew. Chem., Int. Ed.* **2009**, *48*, 6198−6200. (f) Wang, Y. Z.; Quillian, B.; Wei, P. R.; Wang, H. Y.; Yang, X. J.; Xie, Y. M.; King, R. B.; Schleyer, P. V.; Schaefer, H. F.; Robinson, G. H. *J. Am. Chem. Soc.* **2005**, *127*, 11944−11945. (g) Laitar, D. S.; Mathison, C. J. N.; Davis, W. M.; Sadighi, J. P. *Inorg. Chem.* **2003**, *42*, 7354−7356.

(11) (a) Andres, R.; de, J. E.; de, l. M. F. J.; Flores, J. C.; Gomez, R. *J. Organomet. Chem.* **2005**, *690*, 939−943. (b) Kakaliou, L.; Scanlon, W. J.; Qian, B. X.; Baek, S. W.; Smith, M. R.; Motry, D. H. *Inorg. Chem.* **1999**, *38*, 5964−5977.

(12) Tomson, N. C.; Yan, A.; Arnold, J.; Bergman, R. G. *J. Am. Chem. Soc.* **2008**, *130*, 11262−11263.

(13) Tonzetich, Z. J.; Jiang, A. J.; Schrock, R. R.; Müller, P. *Organometallics* **2007**, *26*, 3771−3783.

(14) (a) Chiong, H. A.; Daugulis, O. *Organometallics* **2006**, *25*, 4054−4057. (b) Shimokawa, C.; Itoh, S. *Inorg. Chem.* **2005**, *44*, 3010−3012. (c) Dias, H. V. R.; Flores, J. A. *Inorg. Chem.* **2007**, *46*, 5841−5843. (d) Carrera, N.; Savjani, N.; Simpson, J.; Hughes, D. L.; Bochmann, M. *Dalton Trans.* **2011**, *40*, 1016−1019. (e) Venugopal, A.; Ghosh, M. K.; Jurgens, H.; Tornroos, K. W.; Swang, O.; Tilset, M.; Heyn, R. H. *Organometallics* **2010**, *29*, 2248−2253.

(15) Tian, X.; Goddard, R.; Porschke, K. R. *Organometallics* **2006**, *25*, 5854−5862.

(16) (a) Fekl, U.; Goldberg, K. I. *J. Am. Chem. Soc.* **2002**, *124*, 6804−6805. (b) Fekl, U.; Goldberg, K. I. *Adv. Inorg. Chem.* **2003**, *54*, 259−320. (c) Fekl, U.; Kaminsky, W.; Goldberg, K. I. *J. Am. Chem. Soc.* **2001**, *123*, 6423−6424. (d) Fekl, U.; Kaminsky, W.; Goldberg, K. I. *J. Am. Chem. Soc.* **2003**, *125*, 15286−15287.

(17) (a) Budzelaar, P. H. M.; Moonen, N. N. P.; de Gelder, R.; Smits, J. M. M.; Gall, A. W. *Eur. J. Inorg. Chem.* **2000**, 753−769. (b) Geier, S. J.; Stephan, D. W. *Chem. Commun.* **2008**, 2779−2781.

(18) (a) Bernskoetter, W. H.; Lobkovsky, E.; Chirik, P. J. *Organometallics* **2005**, *24*, 4367−4373. (b) Bernskoetter, W. H.; Lobkovsky, E.; Chirik, P. J. *Organometallics* **2005**, *24*, 6250−6259.

(19) (a) Zhang, J.; Ke, Z.; Bao, F.; Long, J.; Gao, H.; Zhu, F.; Wu, Q. *J. Mol. Catal. A: Chem.* **2006**, *249*, 31−39. (b) Zhou, M.-S.; Huang, S.-P.; Weng, L.-H.; Sun, W.-H.; Liu, D.-S. *J. Organomet. Chem.* **2003**, *665*, 237−245. (c) Yuan, S.; Zhang, L.; Liu, D.; Sun, W.-H. *Macromol. Res.* **2010**, *18*, 690−694. (d) Zhang, D.; Jin, G.-X.; Weng, L.-H.; Wang, F. *Organometallics* **2004**, *23*, 3270−3275. (e) Xue, M.; Jiao, R.; Zhang, Y.; Yao, Y. M.; Shen, Q. *Eur. J. Inorg. Chem.* **2009**, 4110−4188. (f) Van, M. W. J.; Duchateau, R.; Koning, C. E.; Gruter, G.-J. M. *Macromolecules* **2005**, *38*, 7306−7313. (g) Smith, K. M. *Curr. Org. Chem.* **2006**, *10*, 955−963. (h) McGuinness, D. S. Cr Complexes of Nitrogen Donor Ligands for Olefin Oligomerisation and Polymerisation. In *Olefin Upgrading Catalysis by Nitrogen-based Metal Complexes I*; Campora, J., Giambastiani, G., Eds.; Springer: Amsterdam: 2011; Vol. *35*, pp 1−26.

(20) Guan, B.; Xing, D.; Cai, G.; Wan, X.; Yu, N.; Fang, Z.; Yang, L.; Shi, Z. *J. Am. Chem. Soc.* **2005**, *127*, 18004−18005.

(21) (a) Spielmann, J.; Buch, F.; Harder, S. *Angew. Chem., Int. Ed.* **2008**, *47*, 9434−9438. (b) Lazarov, B. B.; Hampel, F.; Hultzsch, K. C. *Z. Anorg. Allg. Chem.* **2007**, *633*, 2367−2373.

(22) (a) Badiei, Y. M.; Dinescu, A.; Dai, X.; Palomino, R. M.; Heinemann, F. W.; Cundari, T. R.; Warren, T. H. *Angew. Chem., Int. Ed.* **2008**, *47*, 9961−9964. (b) Biyikal, M.; Loehnwitz, K.; Meyer, N.; Dochnahl, M.; Roesky, P. W.; Blechert, S. *Eur. J. Inorg. Chem.* **2010**, 1070−1081.

(23) (a) Moreno, A.; Pregosin, P. S.; Laurenczy, G.; Phillips, A. D.; Dyson, P. J. *Organometallics* **2009**, *28*, 6432−6441. (b) Phillips, A. D.; Laurenczy, G.; Scopelliti, R.; Dyson, P. J. *Organometallics* **2007**, *26*, 1120−1122. (c) Phillips, A. D.; Zava, O.; Scopelitti, R.; Nazarov, A. A.; Dyson, P. J. *Organometallics* **2010**, *29*, 417−427.

(24) Rauchfuss, T. *Inorg. Synth.* **2010**, 35.

(25) (a) Carey, D. T.; Cope-Eatough, E. K.; Vilaplana-Mafe, E.; Mair, F. S.; Pritchard, R. G.; Warren, J. E.; Woods, R. J. *Dalton Trans.* **2003**, 1083−1093. (b) Li, Y. F.; Jiang, L.; Wang, L. Y.; Gao, H. Y.; Zhu, F. M.; Wu, Q. *Appl. Organomet. Chem.* **2006**, *20*, 181−186. (c) Phillips, A. D.; Dyson, P. J. Unpublished results.

(26) (a) Fairchild, R. M.; Holman, K. T. *Organometallics* **2008**, *27*, 1823−1833. (b) Fan, L.; Turner, M. L.; Hursthouse, M. B.; Malik, K. M. A.; Gusev, O. V.; Maitlis, P. M. *J. Am. Chem. Soc.* **1994**, *116*, 385−386. (c) Fan, L.; Wei, C.; Aigbirhio, F. I.; Turner, M. L.; Gusev, O. V.; Morozova, L. N.; Knowles, D. R. T.; Maitlis, P. M. *Organometallics* **1996**, *15*, 98−104. (d) Kölle, U.; Kang, B.-S.; Thewalt, U. *J. Organomet. Chem.* **1990**, *386*, 267−273. (e) Yamamoto, Y.; Arakawa, T.; Itoh, K. *Organometallics* **2004**, *23*, 3610−3614.

(27) (a) Kogut, E.; Wiencko, H. L.; Zhang, L.; Cordeau, D. E.; Warren, T. H. *J. Am. Chem. Soc.* **2005**, *127*, 11248−11249. (b) Melzer, M. M.; Jarchow-Choy, S.; Kogut, E.; Warren, T. H. *Inorg. Chem.* **2008**, *47*, 10187−10189.

(28) Chang, S.; Jones, L.; Wang, C.; Henling, L. M.; Grubbs, R. H. *Organometallics* **1998**, *17*, 3460−3465.

(29) Ding, F.; Sun, Y. G.; Monsaert, S.; Drozdzak, R.; Dragutan, I.; Dragutan, V.; Verpoort, F. *Curr. Org. Synth.* **2008**, *5*, 291−304.

(30) Huang, H.; Hughes, R. P.; Rheingold, A. L. *Polyhedron* **2008**, *27*, 734−738.

(31) Koelle, U. *Chem. Rev.* **1998**, *98*, 1313−1334.

(32) (a) Nagashima, H.; Kondo, H.; Hayashida, T.; Yamaguchi, Y.; Gondo, M.; Masuda, S.; Miyazaki, K.; Matsubara, K.; Kirchner, K. *Coord. Chem. Rev.* **2003**, *245*, 177−190. (b) Nagashima, H.; Gondo, M.; Masuda, S.; Kondo, H.; Yamaguchi, Y.; Matsubara, K. *Chem. Commun.* **2003**, 442−443.

(33) (a) Ahlemann, J. T.; Kunzel, A.; Roesky, H. W.; Noltemeyer, M.; Markovskii, L.; Schmidt, H. G. *Inorg. Chem.* **1996**, *35*, 6644−6645. (b) Ahlemann, J. T.; Roesky, H. W.; Murugavel, R.; Parisini, E.; Noltemeyer, M.; Schmidt, H. G.; Muller, O.; HerbstIrmer, R.; Markovskii, L. N.; Shermolovich, Y. G. *Chem. Ber.* **1997**, *130*, 1113−1121. (c) Ahlemann, J. T.; Roesky, H. W.; Noltemeyer, M.; Schmidt, H. G.; Markovsky, L. N.; Shermolovich, Y. G. *J. Fluorine Chem.* **1998**, *87*, 87−90.

(34) (a) Dieck, H. T.; Kollvitz, W.; Kleinwachter, I. *Inorg. Chem.* **1984**, *23*, 2685−2691. (b) Dieck, H. T.; Kollvitz, W.; Kleinwachter, I. *Organometallics* **1986**, *5*, 1449−1457. (c) Nieuwenhuis, H. A.; Stufkens, D. J.; McNicholl, R. A.; Alobaidi, A. H. R.; Coates, C. G.; Bell, S. E. J.; McGarvey, J. J.; Westwell, J.; George, M. W.; Turner, J. J. *J. Am. Chem. Soc.* **1995**, *117*, 5579−5585.

(35) Aarnts, M. P.; Wilms, M. P.; Stufkens, D. J.; Baerends, E. J.; Vlcek, A. *Organometallics* **1997**, *16* (10), 2055−2062.

(36) Kölle, U.; Raabe, G. *Angew. Chem., Int. Ed.* **1993**, *32*, 1294−1294.

(37) Saunders, G. C. *J. Fluorine Chem.* **2010**, *131*, 1187−1191.

(38) Chopra, D.; Row, T. N. G. *Cryst. Eng. Commun.* **2011**, *13*, 2175−2186.

(39) Kalinina, D.; Dares, C.; Kaluarachchi, H.; Potvin, P. G.; Lever, A. B. P. *Inorg. Chem.* **2008**, *47*, 10110−10126.

(40) Kharasch, M. S.; Jensen, E. V.; Urry, W. H. *Science* **1945**, *102*, 128−128.

(41) (a) Matyjaszewski, K. *Curr. Org. Chem.* **2002**, *6*, 67−82. (b) Clark, A. J. *Chem. Soc. Rev.* **2002**, *31*, 1−11. (c) Iqbal, J.; Bhatia, B.; Nayyar, N. K. *Chem. Rev.* **1994**, *94*, 519−564. (d) Minisci, F. *Acc. Chem. Res.* **1975**, *8*, 165−171.

(42) Matsumoto, H.; Nakano, T.; Nagai, Y. *Tetrahedron Lett.* **1973**, 5147−5150.

(43) For reviews about Ru-catalyzed ATRA reactions see: (a) Severin, K. *Curr. Org. Chem.* **2006**, *10*, 217−224. (b) Delaude, L.; Demonceau, A.; Noels, A. F. Ruthenium-promoted radical processes toward fine chemistry. In *Ruthenium Catalysts and Fine Chemistry*; Springer-Verlag: Berlin, 2004; Vol. *11*, pp 155−171. Apart from Ru, Cu and Ni complexes are frequently used for ATRA reactions: (c) Eckenhoff, W. T.; Pintauer, T. *Catal. Rev.-Sci. Eng.* **2010**, *52*, 1−59. (d) Pintauer, T.; Matyjaszewski, K. *Chem. Soc. Rev.* **2008**, *37*, 1087−1097. (e) Gossage, R. A.; Van De Kuil, L. A.; Van Koten, G. *Acc. Chem. Res.* **1998**, *31*, 423−431.

(44) (a) Borguet, Y.; Richel, A.; Delfosse, S.; Leclerc, A.; Delaude, L.; Demonceau, A. *Tetrahedron Lett.* **2007**, *48*, 6334−6338. (b) Quebatte, L.; Haas, M.; Solari, E.; Scopelliti, R.; Nguyen, Q. T.; Severin, K. *Angew. Chem., Int. Ed.* **2005**, *44*, 1084−1088.

(45) (a) Lundgren, R. J.; Rankin, M. A.; McDonald, R.; Stradiotto, M. *Organometallics* **2008**, *27*, 254−258. (b) Quebatte, L.; Scopelliti, R.; Severin, K. *Eur. J. Inorg. Chem.* **2005**, 3353−3358. (c) Simal, F.; Wlodarczak, L.; Demonceau, A.; Noels, A. F. *Tetrahedron Lett.* **2000**, *41*, 6071−6074.

(46) (a) Tutusaus, O.; Delfosse, S.; Demonceau, A.; Noels, A. F.; Vinas, C.; Teixidor, F. *Tetrahedron Lett.* **2003**, *44*, 8421−8425. (b) Tutusaus, O.; Vinas, C.; Nunez, R.; Teixidor, F.; Demonceau, A.; Delfosse, S.; Noels, A. F.; Mata, I.; Molins, E. *J. Am. Chem. Soc.* **2003**, *125*, 11830−11831.

(47) (a) Terasawa, J. I.; Kondo, H.; Matsumoto, T.; Kirchner, K.; Motoyama, Y.; Nagashima, H. *Organometallics* **2005**, *24*, 2713−2721. (b) Motoyama, Y.; Hanada, S.; Niibayashi, S.; Shimamoto, K.; Takaoka, N.; Nagashima, H. *Tetrahedron* **2005**, *61*, 10216−10226. (c) Motoyama, Y.; Gondo, M.; Masuda, S.; Iwashita, Y.; Nagashima, H. *Chem. Lett.* **2004**, *33*, 442−443.

(48) Opstal, T.; Verpoort, F. *Tetrahedron Lett.* **2002**, *43*, 9259−9263.

(49) (a) Bull, J. A.; Hutchings, M. G.; Lujan, C.; Quayle, P. *Tetrahedron Lett.* **2008**, *49*, 1352−1356. (b) Lee, B. T.; Schrader, T. O.; Martin-Matute, B.; Kauffman, C. R.; Zhang, P.; Snapper, M. L. *Tetrahedron* **2004**, *60*, 7391−7396. (c) De Clercq, B.; Verpoort, F. *J. Organomet. Chem.* **2003**, *672*, 11−16. (d) Opstal, T.; Verpoort, F. *New J. Chem.* **2003**, *27*, 257−262. (e) Tallarico, J. A.; Malnick, L. M.; Snapper, M. L. *J. Org. Chem.* **1999**, *64*, 344−345. (f) Simal, F.; Demonceau, A.; Noels, A. F. *Tetrahedron Lett.s* **1999**, *40*, 5689−5693.

(50) Richel, A.; Delfosse, S.; Cremasco, C.; Delaude, L.; Demonceau, A.; Noels, A. F. *Tetrahedron Lett.* **2003**, *44*, 6011−6015.

(51) (a) Wolf, J.; Thommes, K.; Briel, O.; Scopelliti, R.; Severin, K. *Organometallics* **2008**, *27*, 4464−4474. (b) Dutta, B.; Scopelliti, R.; Severin, K. *Organometallics* **2008**, *27*, 423−429. (c) Motoyama, Y.; Hanada, S.; Shimamoto, K.; Nagashima, H. *Tetrahedron* **2006**, *62*, 2779−2788. (d) Quebatte, L.; Scopelliti, R.; Severin, K. *Angew. Chem., Int. Ed.* **2004**, *43*, 1520−1524.

(52) Richel, A.; Demonceau, A.; Noels, A. F. *Tetrahedron Lett.* **2006**, *47* (13), 2077−2081.

(53) Quebatte, L.; Thommes, K.; Severin, K. *J. Am. Chem. Soc.* **2006**, *128* (23), 7440−7441.

(54) (a) Thommes, K.; Fernandez-Zumel, M. A.; Buron, C.; Godinat, A.; Scopelliti, R.; Severin, K. *Eur. J. Org. Chem.* **2011**, 249−255. (b) Fernandez-Zumel, M. A.; Thommes, K.; Kiefer, G.; Sienkiewicz, A.; Pierzchala, K.; Severin, K. *Chem. Eur. J.* **2009**, *15*, 11601−11607. (c) Thommes, K.; Kiefer, G.; Scopelliti, R.; Severin, K. *Angew. Chem., Int. Ed.* **2009**, *48*, 8115−8119. (d) Thommes, K.; Icli, B.; Scopelliti, R.; Severin, K. *Chem. Eur. J.* **2007**, *13*, 6899−6907.

(55) (a) Kamigata, N.; Shimizu, T. *Rev. Heteroat. Chem.* **1997**, *17*, 1−50. (b) Ram, R. N.; Kumar, N. *Tetrahedron Lett.* **2008**, *49*, 799−802. Ram, R. N.; Charles, I. *Chem. Commun.* **1999**, 2267−2268.

(56) Bieniek, M.; Michrowska, A.; Usanov, D. L.; Grela, K. *Chem. Eur. J.* **2008**, *14*, 806−818.

(57) (a) Shriver, D. F.; Drezdzon, M. A. *The Manipulation of Air-Sensitive Compounds*; Wiley-Interscience: New York, 1986. (b) Komiya, S. *Synthesis of Organometallic Compounds: A Practical Guide*; Wiley-Interscience: New York, 1997.

(58) Tilley, T. D.; Grubbs, R. H.; Bercaw, J. E. *Organometallics* **1984**, *3*, 274−278.

(59) (a) Laitar, D. S.; Mathison, C. J. N.; Davis, W. M.; Sadighi, J. P. *Inorg. Chem.* **2003**, *42*, 7354−7356. (b) Li, Y.; Jiang, L.; Wang, L.; Gao, H.; Zhu, F.; Wu, Q. *Appl. Organomet. Chem.* **2006**, *20*, 181−186. (c) Li, Y.; Gao, H.; Wu, Q. *J. Polym. Sci., Part A: Polym. Chem.* **2007**, *46*, 93−101. (d) Hill, M. S.; Pongtavornpinyo, R.; Hitchcock, P. B. *Chem. Commun.* **2006**, 3720−3722.

(60) Dyson, P. J.; McIndoe, J. S. *Inorg. Chim. Acta* **2003**, *354*, 68−74.